ISSN 0347–9226

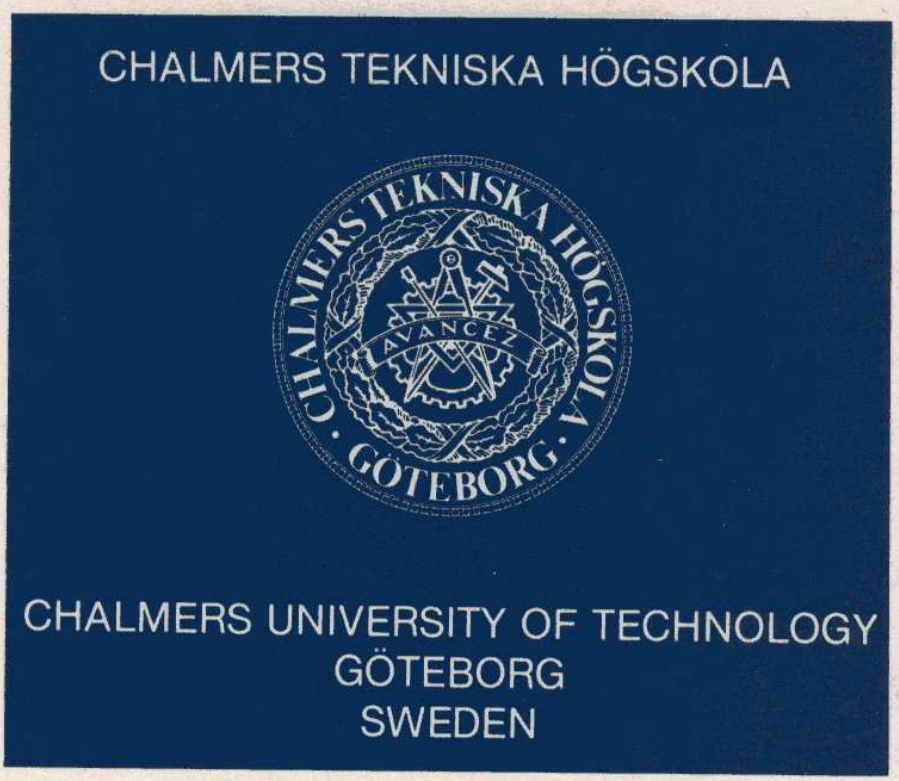

ON THE PROBLEM OF DAMAGE AND LOCALIZATION OF STRAINS

by

V.N. Kukudzhanov, N.G. Bourago, A.N. Kovshov, V.L. Ivanov and D.N. Schneiderman

Publication 95:11

Department of Structural Mechanics
Chalmers University of Technology

1995

Institutionen för Byggnadsmekanik
Chalmers Tekniska Högskola

Chalmers University of Technology
Department of Structural Mechanics
Publication 95:11

ON THE PROBLEM OF DAMAGE AND LOCALIZATION OF STRAINS

by

V.N. Kukudzhanov, N.G. Bourago, A.N. Kovshov, V.L. Ivanov and D.N. Schneiderman

Göteborg 1995

On the problem of damage and localization of strains.

V.N. Kukudzhanov, N.G. Bourago, A.N. Kovshov, V.L.Ivanov, D.N. Schneiderman

Institute for Problems in Mechanics of Russian Academy of Sciences, Moscow, Russia /
Chalmers University of Technology, Structural Mechanics Department,Goteborg, Sweden,

Abstract

A new micro–mechanical model is suggested for investigation of the localization of plastic deformations in shear bands, bands of separation and micro–cracking in semi–brittle materials. In contrast to the usual approach where the plastic deformations and fracture are considered separately, the new approach considers them together as one process of nucleation, growth and coalescence of the micro–defects in materials. The developed model takes into account structural and strain rate effects and gives a macro–constitutive equation that describes damage, relaxation of residual stresses and strain hardening–softening of materials due to structural changing. It is shown on a one dimensional problem of waves propagation in bars (closed form solution) that this model overcomes drawbacks, which the solution based on a strain–softening diagram (Bazant–Belytchko solution) has.
The model is used to study problems of slope stability taking into account strain softening and damage of the materials.
The problem of failure and loss of stability of slopes under gravity forces and a rigid punch pressed on the mass are studied in quasi–static as well as in dynamic formulation. A comparison with classical models using strain softening diagram is made. The results show that the model can be used to describe plastic localization phenomena.

Introduction

The simulation of failure processes in elastic plastic and quasi brittle materials accompanied by localization of plastic deformation that precedes of final fracture is a complicated field of research. Experimental, theoretical as well as numerical simulation difficulties are connected with the physical nature of this phenomena. A deformation process in prefractured state of material is unstable and it is accompanied by transition of a homogeneous state to an essentially nonhomogeneous, as necking, localization in shear bands, bands of separation etc. The classical models and approaches become ill–posed in this situation [1,2].

In the first investigations a real complicated nonhomogeneous prefractured process was replaced by a simple model. In this the usual experimental force–displacement diagrams were mapped onto stress–strain relations. Homogeneity of the stress–strain state was assumed, though it is in strong contradiction to reality. The falling part of the diagram causes an instability of the material. This phenomena is called "strain softening" (Fig.1a).

Many materials reveal strain softening behavior in different processes. In most metals strain softening takes place especially under elevated temperature (Fig.1b). Concrete, soils, rocks are quasi–brittle materials, but they are also characterized by strain softening in micro–cracking and damage processes presided to the fracture [3]. Also some composites show strain–softening behavior. In some materials the strain softening is observed in the phase transformation processes, as carbon–diamonds or martencite–austenite transformation [4]. In dynamics the diagram of the material reveals some parts where the material is softened, but afterwards again becomes hardening [4] (Fig.1c). The approach based on strain softening is convenient because of the great arsenal of methods in classical plasticity. Very soon many defects of this approach were found.

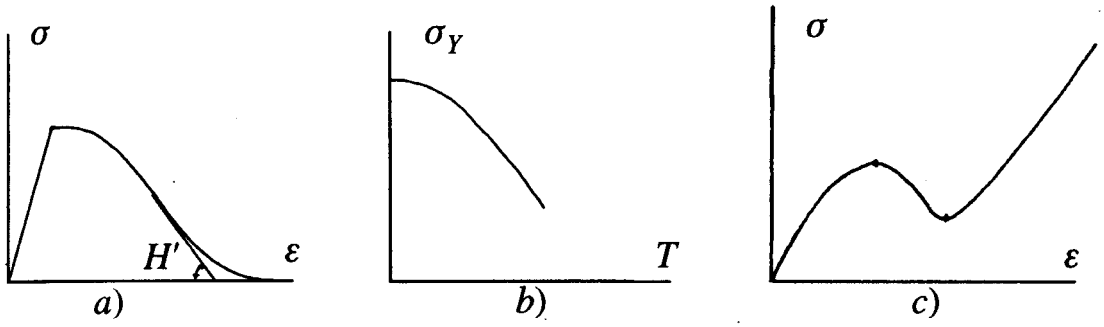

Figure 1. a) Quasi–static strain softening diagram; b) Dependence of yield limit on temperature; c) Dynamic softening diagram.

Classical plasticity for strain–softening materials.

Strain softening plasticity violates Drucker's postulate of material stability

$$d\sigma_{ij}d\varepsilon_{ij} > 0, \tag{1}$$

Obviously this criterion is violated for uniaxial stress state, if strain softening $H = \frac{d\sigma}{d\varepsilon} \le 0$ takes place. In the case of multi–axial strain–stress state the incremental stress–strain relations can be written as

$$d\sigma_{ij} = C_{ijkl}d\varepsilon_{kl}\ , \tag{2}$$

where C_{ijkl} is the tangential stiffness tensor, which depends on stress–strain state. Then the inequality (1) takes the form

$$C_{ijkl}d\varepsilon_{ij}d\varepsilon_{kl} > 0\ . \tag{3}$$

This condition means mathematically the positive–definiteness of the tangential stiffness tensor (condition of ellipticity) and is necessary for the time dependent boundary value problems to be well–posed, otherwise we have an incorrect problem with unstable solution.

We can introduce the explicit dependence of tensor C_{ijkl} on the generalized plastic modules H that is positive, zero or negative for hardening, perfect or softening plasticity, respectively:

$$C_{ijkl} = D^e_{ijkl}\ ,$$

$$C_{ijkl} = D^e_{ijkl} - \frac{1}{A}D^e_{ijpq}g_{pq}f_{mn}D^e_{mnkl}\ , \tag{4}$$

where f_{ij} , g_{ij} are stress derivatives of a yield function f and a plastic potential g and

$$A = H + f_{ij}D^e_{ijkl}g_{kl}$$

Let us denote by H^b the value of the hardening module for which equation (3) is first violated and by H^l the value of the hardening module for which C_{ijkl} becomes singular or $\det C_{ijkl} = 0$. For the associated plasticity $H^l = H^b = 0$; for non–associated plasticity $H^b \ge H^l$ and $H^b > 0$.

In the case of non–associated plasticity the materials are less stable than those in the case of associated plasticity and loss of stability can occur without strain softening. This instability arises due to frictional mechanism of the strength in such materials as sands, rocks, pre–cracked concretes.

Another major problem of classical theory of strain softening is a spurious mesh sensibility in numerical solutions. As it was demonstrated in [6,7] for an example of a simple bar made of strain softening material loaded by uniaxial tension and consisting of several nonhomogeneous elements, the results depend on the discretization of the bar. For an infinite number of elements the post–peak curve "load versus displacement" doubles back on the original loading curve. This mesh sensitivity appears always when the strain rate independent plasticity is used.

There were some attempts to regularize the problem by using a prescribed fracture energy as an additional material parameter [8,9] and defining the softening module H as a function of the element size. In this case the solution of the problem is insensible with respect to mesh refinement, but locally nothing is changed after this "trick" and localization still is the same as before. The numerical simulation with the mesh refinement also encounters some convergence problem and the observation of results shows that the localization strongly depends on the discretization and tends to propagate along the mesh lines. Often obtained patterns of localization are "spurious" and in some cases give occasional jumps from one row of elements to the next and back without any physical motivations [7].

As has been shown analytically for an infinite body and numerically for real boundary value problem the spatial zone, where the ellipticity of the system of governing equations is lost, is of measure zero [2,10]. This spatial zone is a point in one–dimensional problem, a line for two dimensional problem and a surface in the case of three dimensional problem. It seems that this takes away the problem of the incorrectness of the ill–posed boundary value problem. However from one side it is not proved that a correct solution of a boundary value problem exists when the ellipticity is lost in zones of measure zero, and from the other side there are the thermodynamic contradictions due to the absence of dissipation in these cases [10]. The same situation takes place for the dynamic time dependent boundary value problems. A closed form solution was obtained in [10] for the one dimensional impact problem for a strain softening bar. There is only one point where the equations loose the hyperbolicity and become elliptical. The plastic deformation in this point instantly tends to infinity. In all other points of the bar plastic deformation is absent.

So we can see that strain softening applied to classical plasticity is based on the extrapolation assumption of the existence of a stress–strain diagram in the prefractured state which is essentially inhomogeneous. This assumption does not correspond to the reality and obviously leads to the ill–posed boundary value problems.

There are mathematical methods for regularization and solution of this kind of incorrect problems.

Regularization models.

These methods are based on the physical idea that the incorrectness of the model can be overcome by introducing small higher order terms into the governing equations. These terms describe the properties neglected before though they can be essential. These additional terms can be introduced formally as a mathematical regularizations or non–formally using physical imaginations about fracture process. Appropriate models contain higher order differential terms. We can select the non–local damage model [12], the gradient models [13,15] and the Cosserat model [16,17].

Let us briefly discuss the main ideas of some models.

The essential feature of *the gradient plasticity* is that the yield function depends not only on stress σ and strain ε, but also on the higher gradients of ε. For example the yield function can be taken in the form [7]

$$f(\sigma,\varepsilon,\nabla^2\varepsilon) = \sigma - \sigma_s(\varepsilon) - l^2\frac{d\sigma_s}{d\varepsilon}\nabla^2\varepsilon, \tag{5}$$

where l is a material parameter of dimension of length.

For the one dimensional case the equation (5) leads to the equation for the displacements of the bar

$$\varrho\frac{\partial^2 u}{\partial t^2} = \frac{d\sigma_s}{d\varepsilon}\left(\frac{\partial^2 u}{\partial x^2} + l^2\frac{\partial^4 u}{\partial x^4}\right), \tag{6}$$

where $\frac{d\sigma_s}{d\varepsilon} < 0$ for the falling part of the diagram of material. So if $l = 0$ the equation (6) becomes elliptical and problem is incorrect. The additional term restores the hyperbolicity and well posedness of the time–boundary value problem for the equation (6), even if l^2 is a small parameter. In static problems the higher order term restores the ellipticity of the equation. The numerical simulation shows that results are insensitive to mesh refinement [7].

The elasto–visco–plastic model is related to the class with higher order operators in time. For the one dimensional case instead of elastic plastic constitutive equation

$$\sigma = \sigma_s(\varepsilon)\ , \tag{7a}$$

where $\sigma = \sigma_s(\varepsilon)$ is the stress–strain diagram, we have for elastic–visco–plastic material

$$E\frac{\partial\varepsilon}{\partial t} - \frac{\partial\sigma}{\partial t} = \frac{1}{\tau}[\sigma - \sigma_s(\varepsilon)], \tag{7b}$$

where $\tau > 0$ is the material parameter of dimension of time and E is an elastic module. Combining equations (7) with momentum and kinematic equations

$$\varrho\frac{\partial^2 u}{\partial t^2} = \frac{\partial\sigma}{\partial x}\ , \quad \varepsilon = \frac{\partial u}{\partial x}\ , \quad v = \frac{\partial u}{\partial t}$$

we have in the case of elastic plastic material

$$\frac{\partial^2 u}{\partial t^2} - \frac{1}{\varrho}\frac{\partial\sigma_s}{\partial\varepsilon}\frac{\partial^2 u}{\partial x^2} = 0 \tag{8a}$$

and in the case of elastic–visco–plastic material

$$\frac{\partial^2 u}{\partial t^2} - \frac{E}{\varrho}\frac{\partial^2 u}{\partial x^2} = \frac{1}{\tau\varrho}\frac{\partial}{\partial x}(\sigma - \sigma_s(\varepsilon))\,. \tag{8b}$$

The type of the equations (8) is defined by the higher order operator on the left hand side of these equations. If $\frac{\partial\sigma_s}{\partial\varepsilon} < 0$ for the falling part of the material diagram, then the equation (8a) is elliptical and the problem is incorrect. In this case the equation (8b) remains hyperbolic and the problem is correct. If the solution of the equation (8a) has any singularities or discontinuities, for the

equation (8b) ($\tau > 0$) the plasticity is developed as the narrow bands, where the solution has large but finite gradients. At the same time the boundary value problem is well posed if the adequate problem for the elastic material is well posed.

Numerical investigations of the localization show that there is a striking difference between the strain rate independent model (7a) and the strain rate dependent model (7b). Localization for the strain rate dependent model does not proceed along element boundaries or is confined to the row of elements but shows the branching of bands [7]. It should be mentioned that for the elastic–visco–plastic solids a localization bifurcation takes place for higher load compared to the strain rate–independent plasticity. It is so because the modules of bifurcation in elastic–visco–plastic material is elastic. Under isothermal conditions strain rate hardening retards the development of localization since the material stiffens when the strain rate concentrates to the localization bands and smooths them [18]. Nevertheless the phenomenology of the localization in elastic–visco–plastic solids is the same as in rate independent plastic solids.

The basic drawback in using a strain rate dependent model for the regularization of the boundary value problem is that it does not work well for very slow processes and these spurious discretization effects again take place [7]. Perhaps it can mean that the localization of strains appears an essentially dynamic process. However, the considered approach to the investigation of localization of plastic strain by the regularization method has almost the same physical short comings as the model of strain softening in classical plasticity because all considered models with higher order terms do not avoid the general conception of strain softening, but only simplify the numerical calculations or make them more stable.

Micro–mechanical models and its application to the study of localization.

Another way is to take into account the micro–structural changes that take place at a level below the classical continuum level , at the same time not avoiding continuum mechanics approach and phenomenological consideration of the phenomena. Examples of a so called "meso–scopic" approach is a phenomenological theory of dislocation, mechanics of micro–voids and micro–cracks in prefractured solids. This gives the possibility for deeper understanding of the mechanism of the localization.

Now we discuss approaches where the models are based on micro–mechanics of defects. The loss of stress carrying capacity of the materials is allowed as natural outcome of the deformation process, in contrast to the usual approach where plastic deformation and fracture have separative criteria and do not interact with each other.

From micro–mechanical point of view this process can be described as a development of micro–defects, dislocations, micro–cracks and micro–voids, which defines the deformation and damage histories in solids together. One main goal of this approach is to obtain the constitutive equations in the frame of continuum mechanics on the base of equations firstly developed for the micro–parameters such as number of generated voids, rate of its growth etc.

One can put a question: if it is necessary to investigate the micro–level laws, if then we will only ask for their phenomenological consequences? The answer should be positive. As far as micro–mechanical approach not only makes our knowledge deeper, but also gives new information. For example the mathematical modelling of micro–phenomena can show that the problem not al-

ways can be investigated on a macro–level only, since the equations for the micro–parameters and for the macro–parameters can not be separated and should be solved together. Moreover, in the future this can be used to find the ways to construct materials with the prescribed properties.

Certainly both approaches have rights to be developed. Today most of them are phenomenological but new day is coming. Both kinds of models can be represented as the models with internal variables and certainly should satisfy all thermodynamic and general requirements such as objectivity of governing equations, non–negativity of dissipation and so on. The only difference is in the method of the development of these equations.

In recent micro–mechanical models the following properties of micro–defects are introduced: volume (scalar) , orientation (vector) and principal axes for the elliptical voids (tensor) as a measures for its value, shape and rate of the growth [19–25]. The evolution equations are developed from the theoretical solution of the problem for the isolated void embedded in the element of matrix material which is much bigger then the sizes of void and much less than standard size of the body. This means that the solutions are obtained for uniform stresses applied on an infinite body and after that the relations between introduced measures and stresses can be found. The results are presented for both linear and nonlinear materials in a form which will be useful for deriving constitutive equations for voided material. If the matrix medium has a potential, then as it was shown in [23], the voided material has also a potential. Potentials for the isolated voids and cracks are particularly convenient for this purpose. For ellipsoidal voids or elliptical cracks that kind of solution is obtained only for elastic [21,25] and for visco–elastic [20] matrices.

A model of a spherical void in an incompressible perfectly plastic matrix is suggested by Gurson [19]. It allows to obtain the closed form of the yield condition for the perfect plastic material and to develop on this base the phenomenological theory of dilatational plasticity. This theory is widely spread and has several modifications in the latter works [23.25,37].

The observations of metals that fail by the ductile mechanism with localization of plastic deformation in bands reveal that the void volume concentration outside the bands is very low. Some high strength metals display almost complete absence of any voids outside the localization band. This allows to suggest that localization is caused by nucleation of the voids. Small volume concentration of voids can essentially grow in result of the plastic deformation.

A different behavior is displayed by such materials as soil, rock, concrete and certain polycrystalline and multi–phase ceramic materials. They are destructing under tensile loading in a semi–brittle manner. In understanding of this process the nucleation of micro–defects in the regions of residual stress concentration which the phenomena is called micro–cracking [64] very important role plays. Residual stresses together with random orientation of grains give rise to stochastic micro–cracking. The micro–cracking is very useful by producing inelastic adaptivity of material to the brittle fracture.

Here we suggest a new model of continuum failure of elasto–visco–plastic materials based on micro–mechanics of defects. This model describes the hardening–softening effects – both kinematic and isotropic – due to motion of dislocations as well as generation and growth of voids. The thermal softening effects are included, too. The material model is presented in context of small deformations.

1. Constitutive equations based on micro–mechanics.

Here we suggest the strain rate dependent theory of damage processes in elastic plastic medium based on micro–mechanics.

1.1. Models of plasticity based on dislocation theory.

The rate–independent constitutive equations for the plastic media with initial spherical voids were presented by Gurson [19]. The version of the Gurson model taking into account nucleation of the voids was introduced in [34].

The strain rate dependent constitutive equations for softening material were used for the consideration of localization effects in [34–36] without consideration of micro–defects and damage of the material. In [37] a strain rate dependent and damage model with finite deformations were suggested for modelling the dynamic failure processes. The rate sensitive version of Gurson's theory were introduced by Pan, Salje and Needlemann [34] and then the localization processes were considered in [35–37], but only for isotropic hardening materials and with phenomenological equation for the scalar parameter of porosity. Another point is that this theory, as well as Gurson's, did not consider the mechanism of generation of voids and had not criteria for the appearance of voids.

Here we try to introduce the model taking into account the whole process of rate dependent plastic deformation consisting from two stages: one before the generation of micro–cracks and another after that, both based on micro–mechanical approach.

1.2. Dislocations and plastic strains.

It should be noted that material constants obtained from micro experiments can not be used in the macro equations for the modelling of the processes of plastic deformation. Some corrections are required on the base of macro experiments. Micro–mechanics gives us the general structure of the constitutive equations.

In order to describe the process of generation of micro–defects we separate the full dislocation flux $\dot{p}_{ij}$ into two parts

$$\dot{p}_{ij} = \dot{\varepsilon}^p_{ij} + \dot{d}_{ij} \,. \tag{1.1}$$

First part is responsible for plastic deformation, second part represents the dislocations accumulated on the boundaries of grains and converted into micro–cracks.

Let σ_{ij} be a stress, $\sigma^r_{ij} = \varkappa \varepsilon^p_{ij}$ be a residual stress and $\sigma^a_{ij} = \sigma_{ij} - \sigma^r_{ij}$ be an active stress. Factor $\varkappa$ is a Baushinger's parameter. Micro–mechanics shows [38–40] that plastic flow begins only if the intensity of active stress $S^a = (\sigma'^a_{ij}\sigma'^a_{ij})^{1/2}$ reaches the critical value s^a_0 and the intensity of the plastic strain rate $\dot{E}^p = (\dot{\varepsilon}_{ij}\dot{\varepsilon}_{ij})^{1/2}$ depends on the value of $S^a - s^a_0$:

$$\tau_p \dot{E}^p = \psi_p(S^a - s^a_0) \tag{1.5}$$

where τ_p and ψ_p are the relaxation time and relaxation function. In the case of quasi–static processes when $\tau_p \dot{E}^p \to 0$ the dependence (1.5) tends to the yield condition of the time independent theory.

We can take the hardening function s_0^a for example according to Garson's theory, where this function was found from the approximate solution of the problem for spherical void in a perfectly plastic material loaded by remote forces. This expression in generalized form is

$$s_0^a = \sigma_s \sqrt{1 + q_1^2\gamma^2 - 2\gamma q_1 \, ch(\frac{3q_2}{2}\frac{\sigma_{kk}}{\sigma_s})} . \tag{1.6}$$

where $\sigma_s = \sigma_s(E_p)$ is the yield limit, γ is a porosity, q_1 , q_2 are parameters introduced to improve the accuracy of the model (in original solution they were unity).

From the continuity equation it is easy to derive the equation for the porosity

$$\dot{\gamma} = (1 - \gamma)\dot{\varepsilon}^p_{kk}, \tag{1.7}$$

We suppose that plastic strain rate is subjected to the flow rule associated with potential $F_p = S^a - s_0^a + \psi_p^{-1}(\tau_p \dot{E}^p)$, then

$$\dot{\varepsilon}^p_{ij} = \Lambda_p \frac{\partial F_p}{\partial \sigma_{ij}} , \quad \Lambda_p = \frac{\psi_p(S^a - s_0^a)}{\tau_p S^a} \tag{1.8}$$

Taking into account Hooke's law

$$\dot{\sigma'}_{kl} = 2\mu(\dot{\varepsilon'}_{kl} - \dot{\varepsilon'}^p_{kl}) , \quad \dot{\sigma}_{kk} = 3K(\dot{\varepsilon}_{kk} - \dot{\varepsilon}^p_{kk}) \tag{1.9}$$

from equations (1.6),(1.8)–(1.9) we come to the constitutive equations for stresses :

$$\dot{\sigma'}_{kl} = 2\mu\left(\dot{\varepsilon'}_{kl} - \frac{\psi_p(S^a - s_0^a)}{\tau_p S^a}\sigma'^a_{kl}\right) , \tag{1.10}$$

$$\dot{\sigma}_{kk} = 3K\left(\dot{\varepsilon}_{kk} - \frac{\psi_p(S^a - s_0^a)}{\tau_p S^a}\frac{3\gamma q_1 q_2}{\sigma_s} sh\frac{3q_2\sigma^a_{kk}}{2\sigma_s}\right) , \tag{1.11}$$

Equation for porosity (1.7) now can be written as

$$\dot{\gamma} = (1 - \gamma)\dot{\varepsilon}^p_{kk} = \frac{\psi_p(S^a - s_0^a)}{\tau_p S^a}\frac{3\gamma(1 - \gamma)}{T_s} q_1 q_2 sh\frac{3q_2\sigma_{kk}}{2T_s} \tag{1.12}$$

1.3. Damage.

We assume that the process of generation of the micro–voids and micro–cracks will begin only if the intensity of the stress $S = (\sigma_{ij}\sigma_{ij})^{1/2}$ reaches the critical value s_0^r . The intensity of the damage $\dot{D} = (\dot{d}_{ij}\dot{d}_{ij})^{1/2}$ depends on the value of $S - s_0$

$$\tau_d \dot{D} = \psi_d(S - s_0), \tag{1.13}$$

where τ_d and ψ_d are the relaxation time and relaxation function.

We suppose that the flux of damage $\dot{d}_{ij}$ is subjected to the flow rule associated with potential $F_d = S - s_0 + \psi_d^{-1}(\tau_d \dot{D})$, then

$$\dot{d}_{ij} = \Lambda_d \frac{\partial F_d}{\partial \sigma_{ij}} \ , \quad \Lambda_d = \frac{\psi_d(S - s_0)}{\tau_d S^r} . \tag{1.14}$$

The relaxation functions ψ_p and ψ_d equal to zero for negative values of their arguments.

1.4. Influence of micro–defects on the elastic properties of materials

That the influence of micro–defects on elastic modules can be neglectful is not true for the semi–brittle materials like some geo–materials, ceramics and some composites. Elastic and dissipation deformations in these materials have another nature, different from metals. Instead of dislocation mechanism they have micro–cracks growth and a nucleation mechanism from the beginning of the deformation process. The micro–defects in these materials have highly random distribution and material remains isotropic and only changes his elastic modules during the deformation. In many cases this effect is significant and plays an important role in applications.

As it was mentioned above in the review there exists an extensive literature on the microscopic properties of voided elastic solids. They can be obtained theoretically from micro–scopic consideration from an isolated micro–defect solution, as well as from macro–experiments with the damaged material. One of those methods is connected with the measurements of wave propagation rates for the different levels of damage and porosity in the following form [65,66]:

$$c_1^2 = \frac{(\lambda_0 + 2\mu_0)}{\varrho_0} f_1(\gamma, D) \ , \quad c_2^2 = \frac{2\mu_0}{\varrho_0} f_2(\gamma, D) \ ,$$

Influence of damage on the yield limit also should be taken into account.

1.5. Discussion.

In order to make clear the main features of the suggested model it is convenient to consider the geometric representation of yield surfaces in the stress space commonly used in theory of plasticity.

It should be noted that the real processes according to our model do not take place in stress space but in an extended space of internal variables, but we can discuss the mapping of this processes in stress space schematically.

There are two surfaces in stress space,defined by equations $F_p = 0$ and $F_d = 0$. Both of them are spherical with radii that depend on the strain rate $\dot{E}^p$ and rate of the damage. These potential surfaces are non–stationary but they have limiting positions which are independent on rates $S = s_0$ and $S^a = s_0^a$. We call them limiting stationary surfaces. These stationary surfaces detect the change of the deformation phases. Stationary surfaces $S^a = s_0^a$ separate the region of elastic deformation from the viscoplastic and $S = s_0$ the region of crackless plastic deformation from (plastic or elastic) deformation with micro–cracks.

Inside the surface $S^a = s_0^a$ the material is elastic, outside it becomes visco–plastic. The elastic and plastic behavior of material depends on damage, which is grows outside the stationary surface $S = s_0$. So the model fully describes hardening – softening processes in strain rate dependent materials.

The constitutive equations do not lose their hyperbolicity in dynamic problems and ellipticity in the statics nor in the first neither in the second stage of deformation, then the generation of voids

begins. The main differential operator of the governing equations remains elastic both in the first and in the second stage. All problems that are well–posed for elastic material in static and dynamics will stay well–posed for the suggested model not only for hardening, but also for strain softening materials due to the fact that plastic properties are included only in low order terms of the equations. Also the damage process is allowed for pure elastic materials.

If the maximal relaxation time τ_p , $\tau_d \ll t_0$, where t_0 is the total time of the process, our equations tend to the strain rate independent ones for which the time boundary problems are ill–posed. For small (but finite) τ_p , τ_d the time boundary problems are still well posed and our model can be considered as a regularization of the strain rate independent governing equations. The accurate proof of this statement was made for the plastic stage of the process in [45] and [67].

It should be emphasized that the significance of this model is not exhausted only by regularization of known equations, as far as it takes into account other effects that are not considered by Gurson's theory. One of them is the generation of micro–cracks during the deformation.

2. One–dimensional wave propagation in a bar.

Before modelling two or three dimensional problems based on the suggested equations a one–dimensional solution should be considered, since in this simple case a close form solution is available , that can make clear the properties of the solution and features of the investigated phenomena.

2.1. Formulation of problem.

Let us consider a bar of length $2L$, with unit cross section and mass ϱ per length. Let the bar be loaded by forcing both ends to move with constant opposite velocity of magnitude v_0 . Due to symmetry of the problem only the right hand side of the bar $x > 0$ (Figure 2.1a) can be taken in to account.

The equivalent problem takes place for a bar with fixed end at $x = 0$. This problem for a strain softening and strain rate insensitive material (Figure 2.1b) was solved by Bazant and Belitchko [10] in closed form. It was shown that localization can occur in one point $x = 0$ where the strain goes to infinity and the stress in this section drops to zero instantly. The solution give regardless of the shape of strain softening diagram, that the total dissipation is found to vanishes. So the solution has some short comings. They could be overcome, if we consider this problem on the base of the suggested strain rate dependent model.

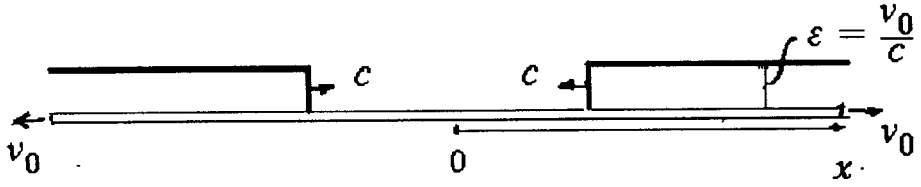

Figure 2.1a The distribution of deformation along the bar [10] for $t < \frac{L}{c}$.

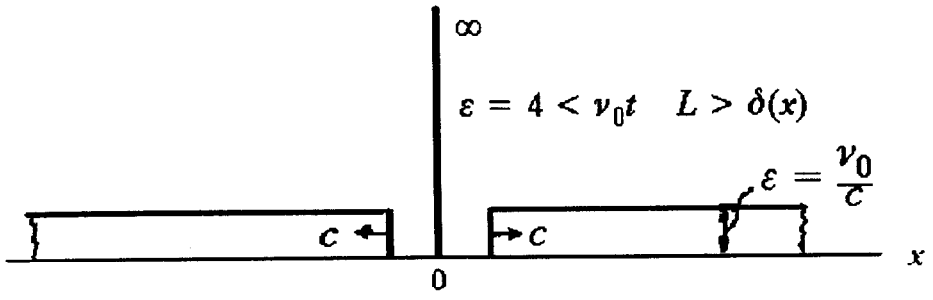

Figure 2.1b The distribution of deformation along the bar [10] for $t > \frac{L}{c}$.

We consider this problem using the strain rate dependent equations taking into account the influence of damage on elastic module. The behavior of the material under quasi–static extension is shown on Figure 2.2.

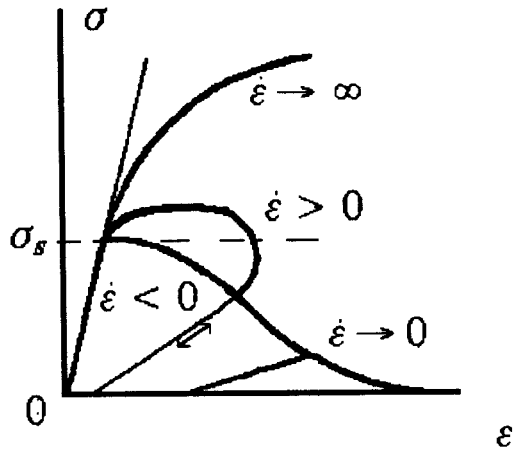

Figure 2.2 $\sigma - \varepsilon$ curves at different strain rates for equations (2.1c),(2.1d).

The system of equations is

$$\varrho_0 \frac{\partial v}{\partial t} = \frac{\partial \sigma}{\partial x} \ , \tag{2.1a}$$

$$\frac{\partial \varepsilon}{\partial t} = \frac{\partial v}{\partial x} \ , \tag{2.1b}$$

$$\frac{\partial \sigma}{\partial t} = E(D)\frac{\partial v}{\partial x} - \frac{1}{\tau} < [\sigma - \sigma_s(\varepsilon)] >^n \ , \quad n > 0 \tag{2.1c}$$

$$\frac{\partial D}{\partial t} = \frac{D_0}{\tau_0} < [\sigma - \sigma_s(\varepsilon)]^n > \ . \tag{2.1d}$$

where τ and τ_0 are the relaxation times for plastic flow and for damage process.
The initial and boundary conditions are

$$t = 0 \ , \quad \vec{U} = 0; \tag{2.2a}$$

$$x = 0 \ , \quad v = 0; \tag{2.2b}$$

$$x = L\ , \quad v = v_0 H(t)\ , \tag{2.2c}$$

where $H(t)$ denote the unit step function and D is a scalar damage parameter.

2.2. Solution of problem.

The system (2.1) can be written in matrix form as

$$\frac{\partial \vec{U}}{\partial t} + A(\vec{U})\frac{\partial \vec{U}}{\partial x} = \vec{F}(\vec{U})\ , \tag{2.3}$$

where $\vec{U} = \vec{U}(v, \varepsilon, \sigma, D)$ is a vector of unknowns. The matrix $A(\vec{U})$ and the vector $\vec{F}(\vec{U})$ can be easily obtained from (2.1).

The eigen values of the matrix $A(\vec{U})$ are

$$\det |A(D) - \lambda I| = 0\ , \quad \lambda_{1,2} = \pm \left(\frac{E(D)}{\varrho_0}\right)^{1/2}\ , \quad \lambda_{3,4} = 0 \tag{2.4}$$

The type of system of equations (2.1) remains hyperbolic for any diagram of strain hardening or strain softening $\sigma = \sigma_s(\varepsilon)$.

The characteristic relations are easily found

$$dx \pm \lambda_{1,2}(D)dt = 0\ , \quad E(D)dv \mp d\sigma = \frac{1}{\tau} < (\sigma - \sigma_s(\varepsilon))^n > dt \tag{2.5a}$$

$$dx = 0 \quad E(D)d\varepsilon - d\sigma = \frac{1}{\tau} < (\sigma - \sigma_s(\varepsilon))^n > dt \tag{2.5b}$$

$$dx = 0 \quad dD = \frac{D_0}{\tau_0} < (\sigma - \sigma_s(\varepsilon))^n > dt \tag{2.5c}$$

If $\sigma < \sigma_s(\varepsilon)$ then vector $\vec{F}(\vec{U}) \equiv 0$

$$\frac{\partial D}{\partial t} = 0 \qquad D = D_* > 0 \qquad \lambda_{1,2}(D_*) < \lambda_{1,2}(0) \tag{2.5d}$$

If $\sigma < \sigma_s(\varepsilon)$ in section $x = x_0$ for $t > 0$ then $\lambda_{1,2} = \pm \left(\frac{E_0}{\varrho}\right)^{1/2}$, where E_0 is the module of undamaged material.

The solution of the problem (2.1)–(2.2) can be obtained numerically using characteristics and relations along them (2.5) [39]. The characteristic method allows obtaining the solution qualitatively by geometrical consideration in the xt–plane and gives all the main features of solution.

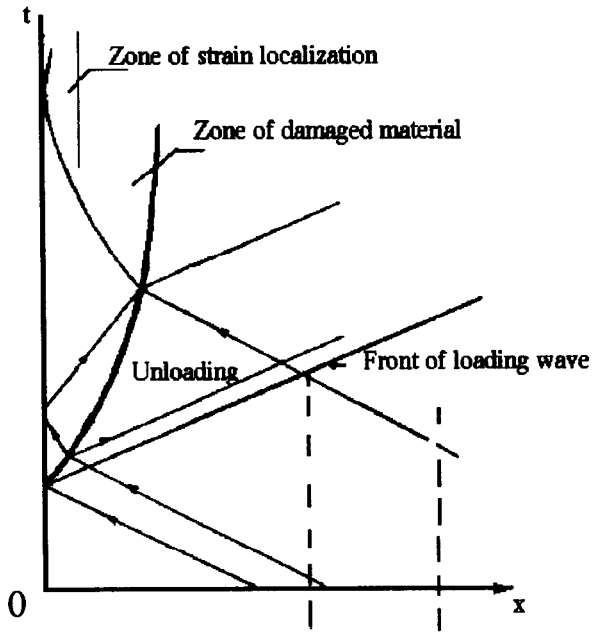

Figure 2.3a. Patterns of characteristic in x–t plane.

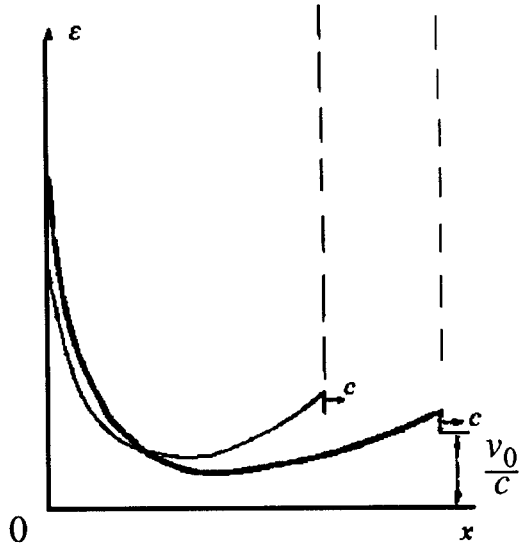

Figure 2.3b. Distribution of deformation along a bar.

The solution is shown in Figure 2.3. The elastic wave emanating by an applied velocity v_0 at $x = \pm L$ is propagating to the midpoint of the bar $x = 0$. When the waves meet each other at $x = 0$ the stress and the strain are doubled. In result in the section $x = 0$ and near it the condition $\sigma > \sigma_s(\varepsilon)$ is satisfied and damage develops. The speeds of disturbances $\lambda_{1,2}$ are decreased and became less than in elastic part $\lambda^{(i)}(D) < \lambda^{(i)}(0)$, $i = 1,2$. This leads to particular wave reflection from the boundary between damaged and elastic parts of the bar. The wave of loading propagates into the damaged part of the bar (Figure 2.3a). The damage and deformation are progressively increased near the section $x = 0$, the energy of the applied impulse is concentrated in the region of damage. The distribution of deformation along the bar for the different moments of time is shown in Figure 2.3b . The deformation is localized in point $x = 0$ the elas-

tic unloading wave is spread to the right side of the bar and the amplitude of the discontinuity wave attenuates.

2.3. Qualitative investigation of localization band.

It is possible to obtain the qualitative values of the deformation and damaged band width and their changes during time in closed form for $t >> \tau$ $(\tau > \tau_0)$. Let us introduce the dimensionless variables

$$\tilde{x} = \frac{x}{c_0 t_0}\ ,\quad \tilde{t} = \frac{t}{t_0}\ ,\quad \tilde{v} = \frac{v}{v_0}\ ,\quad \tilde{\sigma} = \frac{\sigma}{\sigma_0}\ ,\quad \tilde{D} = \frac{D}{D_0} \tag{2.7}$$

where $c_0 = \left(\frac{E_0}{\varrho_0}\right)^{1/2}$, $t_0 = \frac{L}{c}$, $\delta = \frac{\tau}{t_0} << 1$. We shall for simplicity restrict ourselves to the case the static module $E = E_0$ does not depend on D. The dimensionless form of equations (2.1) is

$$\frac{\partial \tilde{\sigma}}{\partial \tilde{x}} = \frac{\partial \tilde{\varepsilon}}{\partial \tilde{t}}\ ,\quad \frac{\partial \tilde{\varepsilon}}{\partial \tilde{x}} = \frac{\partial \tilde{v}}{\partial \tilde{t}}\ , \tag{2.8a}$$

$$\delta\left(\frac{\partial \tilde{\varepsilon}}{\partial \tilde{t}} - \frac{\partial \tilde{\sigma}}{\partial \tilde{t}}\right) = \left[|\tilde{\sigma}| - \sigma_s(\tilde{\varepsilon})\right]^n\ ,\quad \delta\frac{\partial \tilde{D}}{\partial \tilde{t}} = \left[|\tilde{\sigma}| - \sigma_s(\tilde{\varepsilon})\right]^n \tag{2.8b}$$

The tilde above the letters will be omitted.

We shall seek a solution of equations (2.8) as a power expansion in a small parameter δ

$$\vec{U} = \vec{U}^{(0)} + \delta\vec{U}^{(1)} + O(\delta^n)$$

After substitution into (2.8) we get for the zero approximation

$$\frac{\partial v^{(0)}}{\partial t} = c^2(\varepsilon^{(0)})\frac{\partial \varepsilon^{(0)}}{\partial x}\ ,\quad \frac{\partial \varepsilon^{(0)}}{\partial t} = \frac{\partial v^{(0)}}{\partial x}\ ,\quad c^2(\varepsilon) = \frac{d\sigma_s(\varepsilon)}{d\varepsilon}\ .$$

Excluding $v^{(0)}$, we get the nonlinear wave equation

$$\frac{\partial^2 \varepsilon^{(0)}}{\partial t^2} = c^2(\varepsilon^{(0)})\frac{\partial^2 \varepsilon^{(0)}}{\partial x^2}\ , \tag{2.9}$$

where $c^2(\varepsilon)$ changes the sign: in the elastic region it is positive and in strain softening it becomes negative as for the strain rate independent theory.

It is well known that when localization takes place in the stress softening elliptical region the gradients of solution are very high. This contradicts the assumption of smoothness of solution that was made to obtain (2.8), so they are not valid at the region where localization takes place. In this region it must be taken into account that derivatives over x are large, and we must introduce another small parameter λ, which characterizes the rate of solution change in the vicinity of localization, and change the scale of variable x as

$$\beta = \frac{x}{\lambda} \tag{2.9}$$

Parameter λ should be defined from the solution of the problem. Now we take the expansion over a parameter λ of the following kind

$$v = v^{(0)} + \lambda v^{(1)} + \ldots + O(\lambda^n) , \tag{2.10a}$$

$$\sigma = \sigma_s(\varepsilon) + \lambda\sigma^{(1)} + \ldots + O(\lambda^n) , \tag{2.10b}$$

$$\varepsilon = \frac{1}{\lambda}\varepsilon^{(0)} + \lambda\varepsilon_1 + \lambda\varepsilon_2 + \ldots + O(\lambda^n) , \tag{2.10c}$$

For the zero approximation instead of (2.9) we obtain the following equations

$$\frac{\partial v^{(0)}}{\partial t} = b\frac{\partial}{\partial\beta}\left(\frac{\partial v^{(0)}}{\partial\beta}\right)^{1/n} , \quad \frac{\partial v^0}{\partial\beta} = \frac{\partial\varepsilon^0}{\partial t} , \quad \lambda = \delta^{-(n+1)} . \tag{2.11}$$

The boundary conditions for the equation (2.11) are found from the coalescence conditions with the slowly changing solution of the equation (2.9) in the hyperbolic region. Since the elastic wave of amplitude $v = v_0$ is propagated to the direction $\beta > 0$, we can obtain

$$v|_{\beta=0} = 0 , \quad v|_{\beta\to\infty} = v_0 \tag{2.12}$$

The initial conditions do not play any role because solution is valid for $t \gg \tau$, the only requirement is – they should not be in contradiction with conditions (2.12). The problem (2.11)–(2.12) has an automodel solution depending only on variables $z = \frac{\beta}{t^{\frac{n}{n+1}}}$. The equation (2.11) becomes the ordinary differential equation

$$\frac{d^2v}{dz^2} + \frac{b\beta^2 z}{p+1}\left(\frac{dv}{dz}\right)^{p+2} = 0 \tag{2.13}$$

For $n = 1$ the solution is

$$v = \frac{2v_0}{\sqrt{\pi}}\int_0^z e^{-\xi^2}d\xi \tag{2.14a}$$

if $n > 1$

$$v = \frac{v_0}{I_1}\int_0^\xi \frac{dz}{(1+z^2)^{|p|}} , \quad p = \frac{n}{1-n} , \quad n > 0 \tag{2.14b}$$

where

$$I_1 = \int_0^\infty \frac{dz}{(1+z^2)^{|p|}} = \frac{\Gamma(1/2)\Gamma(|p| - 1/2)}{2\Gamma(|p|)} , \tag{2.14b}$$

$$\xi = z\left|\frac{n(1-n)}{1+n}\right|^{1/2}\left(\frac{v_0}{I_1}|\beta|\right)^{\frac{1}{2|p|-1}} . \tag{2.14b}$$

For $n < 1$ the width of the localization band over variable z has finite size z_0 and instead of conditions (2.12) we should take the boundary conditions over the interval $[0, z_0]$

$$v(0) = 0\ , \quad v(z_0) = v_0\ , \quad v'(z_0) = 0\ . \tag{2.15}$$

We have then the solution of the problem (2.13)–(2.15) for $n < 1$

$$v = \frac{v_0}{I_0}\int_0^{\frac{z}{z_0}} (1 - \xi^2)^p d\xi\ , \quad I_0 = \frac{\Gamma(p+1)\Gamma(\frac{1}{2})}{2\Gamma(p+\frac{3}{2})} \tag{2.14c}$$

For $n \geq 1$ we can introduce the effective width of localization band according to the formula

$$\Delta x = \frac{v_0}{\max\left(\frac{dv}{dx}\right)} = \left(\frac{t}{\tau}\right)^{\frac{n}{n+1}} \Delta z \tag{2.16}$$

where Δz is the effective width over the z coordinate.

For $n = 1$ it gives

$$\Delta x = \left(\frac{2\pi t}{\tau}\right)^{1/2} \tag{2.17a}$$

and

$$\varepsilon \approx A\left(\frac{t}{\tau}\right)^{1/2} \tag{2.17b}$$

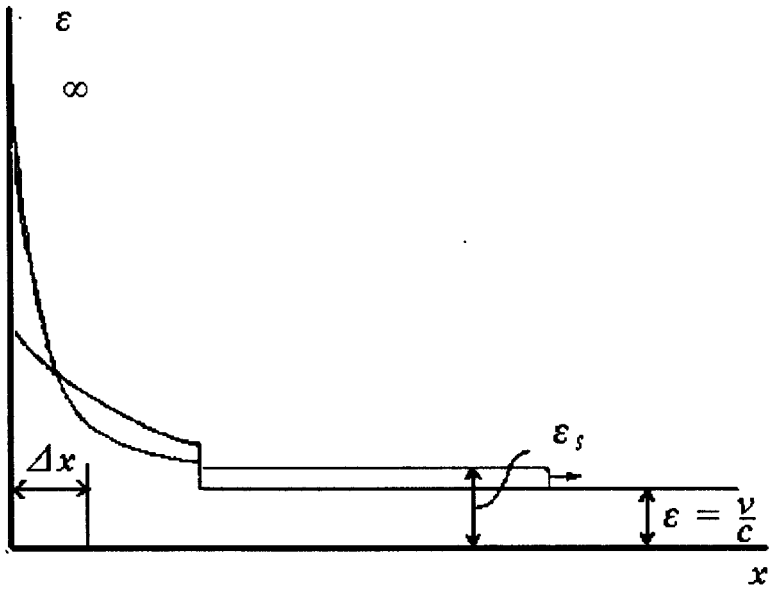

Figure 2.4 Distribution of deformation along a bar for $t \gg \tau$ and for constant elastic modules $E = E_0$ at two times t_1 and t_2 $(t_2 > t_1)$. Here Δx is an effective width of localization zone.

The distribution of ε along a bar is shown an the Figure 2.4 at different time of t. Comparing this solution to the Bazant–Belitchko solution [10] we see that the deformation is localized not to one point but in the band width Δx which grows slowly with time. The deformation inside the band tends to infinity $\varepsilon \to \infty$ $(t \to \infty)$ according to formula (2.16). So the obtained solution has the same main feature as the Bazant–Belitchko solution: localization in the midpoint of the bar, but it has not shortcomings such as zero dissipation.

3. Quasi–static stability of slope under punch pressure

Investigation of failure of slopes has many applications in mining industry ,where it often is connected often with catastrophic accidents [57].

This phenomenon has been extensively investigated by mathematical simulation, as well as by experimental methods [28,46,47]. Difficulties met in this problem are due to transition of large mass of soil from unstable equilibrium to accelerated motion under release of accumulated potential energy.

Theoretical investigation of this problem is based on the theory of plasticity. Initially the rigid plastic analysis was applied to this problem [46,47]. Later elastic plastic models was used for the case of small deformations [48,49,50] that allow studying only the pre–failure stage of process and only in quasi–static formulation.

In recent works the problem is analyzed within the concept of strain softening rate independent plasticity. The difficulties appeared at numerical modelling using the finite element method are discussed in papers [49,52,58] and special methods are suggested to overcome them in [31,57,53,54].

3.1. Formulation of problem.

A quasi–static plane strain problem of stability of the slope under the punch is considered (see Figure 3.1). The boundaries BC and CD are fixed, AD and BH are free. The pie of the boundary under the punch AH is free from the traction and moves down with permanent velocity.

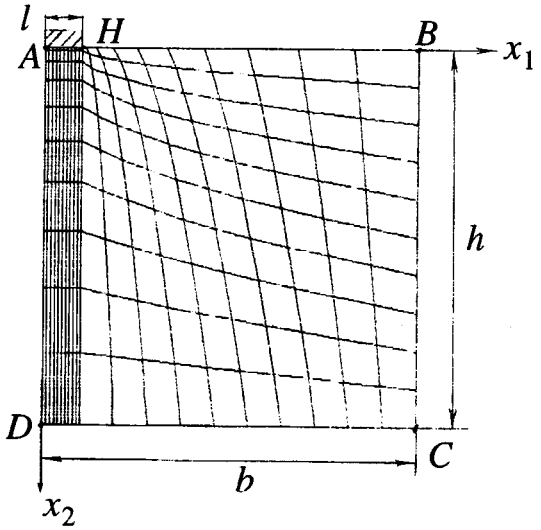

Fig.3.1. A vertical slope under punch pressure. A finite element mesh.

The material is strain–softening and voided. The elastic properties are: $\nu = 0.33$ (Poisson's ratio) and $E = 769 s_0^a$ (Young's module). Two models were compared. One taking into account

damage of nucleated spherical voids with the coefficients $q_1 = q_2 = 1$ and perfectly plastic material, another model – strain softening material with coefficients $q_1 = q_2 = 0$ and softening diagram $S^a = s_0^a(1 - E^p)$. Parameter $\varkappa = 0$ in both cases.

At the beginning of the process the slope is free from stresses and porosity.

3.2. Method of solution

The finite element method has been used. A mesh of 4– and 8– nodal isoparametric elements is shown on Figure 3.1. The integration over the element is done numerically by Gaussian formula with 2 and 4 points of integration along each coordinate respectively. All the unknowns were calculated in nodes after each increment of the punch displacement using quasi–Newtonian incremental scheme.

3.2. Results.

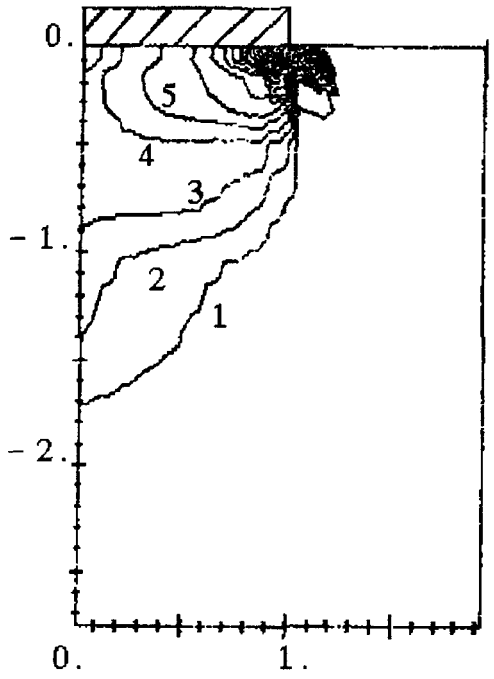

Figure 3.2 Perfectly plastic material with nucleated spherical voids. Contour lines of Odquist parameter ($N = 29$).

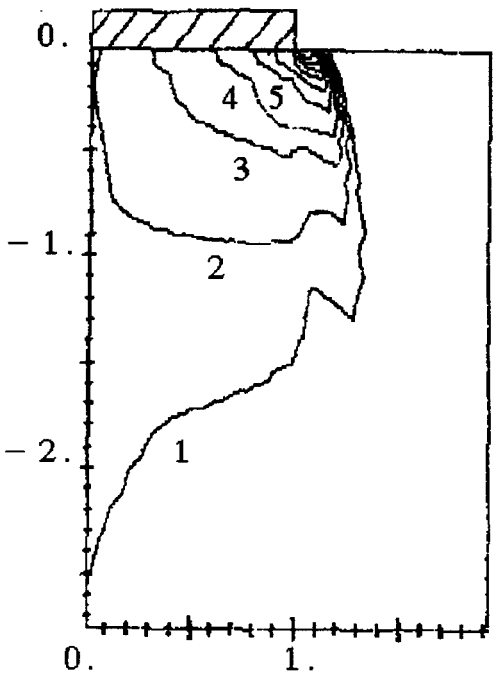

Figure 3.3 Strain softening model. Contour lines of Odquist parameter ($N = 10$).

On the Figures 3.2 and 3.3 contour lines of the Odquist parameter E_p are given for the two models of the material for the maximal displacement of punch $d = 0.045l$. The step of contour lines is $\Delta\varepsilon_p = 0.009$, N is a number of lines. The deformation according to the first model (27%) is three times more that for the second model (9%). For the first model the larger localization is observed in vicinity of the right side corner of the punch.

The dependence between the dimensionless force on the punch and the displacement for the first model (curve 1) and for the second model (curve 2) is given on Figure 3.4.

For small values $\frac{d}{l} \leq 0.008$ the curves coincide, but for higher values the curve 1 is decreased more than 20% from the maximum while the curve 2 shows the increase more than 50% until

the iteration process is convergent. The loss of convergence was happened at the 45th step of incremental procedure.

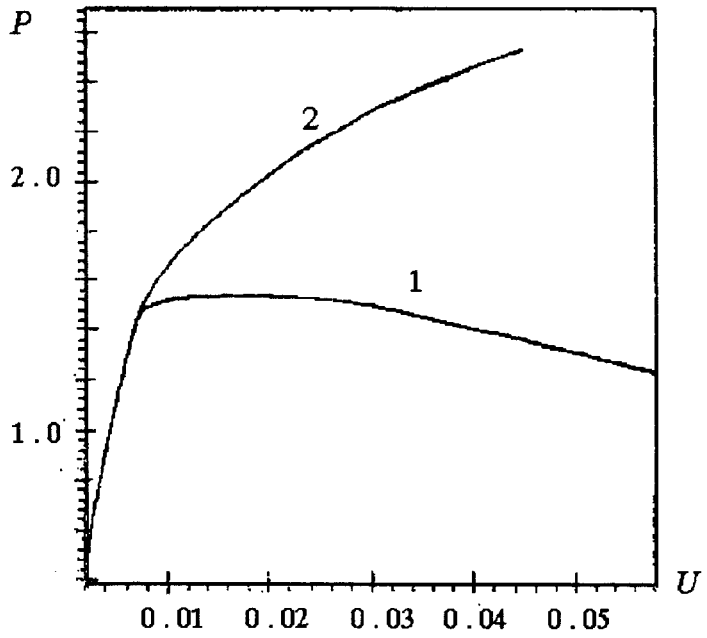

Figure 3.4. The dimensionless force of the punch pressure $P/(l\tau_s^0)$ versus the punch displacement $\frac{d}{l}$ for the model with damage (1) and for the strain softening model (2).

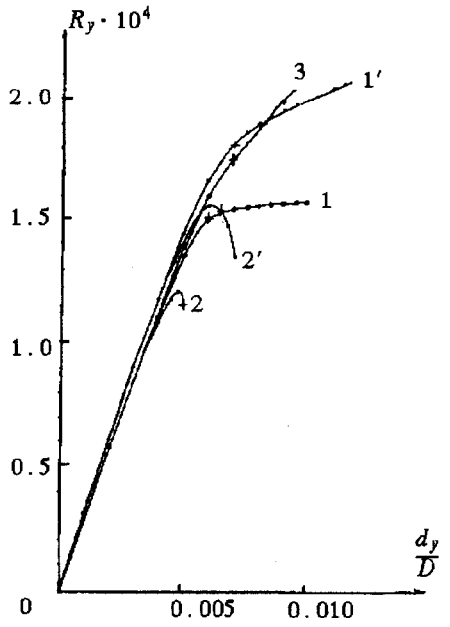

Figure 3.5 Spurious mesh effect for force versus displacement curves for perfect plasticity and for strain softening models:
$1' - H' = 0$, $4 -$ *nodes*; $1 - H' = 0$, $8 -$ *nodes*;
$2' - H' < 0$, $4 -$ *nodes*; $2 - H' < 0$, $8 -$ *nodes*;
$3 - H' > 0$, $8 -$ *nodes*; $+ - d^*$.

For the first model there were no signs of violation of convergence, the calculation were continued until 60–th step and then stopped. That means there is the sign of the presence of a spurious mesh effect in the numerical results for strain rate independent strain softening model. This was confirmed by calculation with mesh refinement and by using the eight nodal elements. The results is shown on Figure 3.5. The increasing accuracy of calculation are decreasing the critical value of force and drop of the curve is abrupt. That confirms the results of other authors [7,49]. For the first model this effect was not observed.

The conclusion can be made the model with micro–voids gives better results and may be used for the description of the localization phenomena in strain softening materials.

4. Dynamics of slope under weight forces.

Let us consider the failure of a slope under gravity.

4.1. Formulation of the problem.

Here we use a dynamic formulation of the problem since small disturbances cause the rather fast sliding of a large mass along shear bands [56]. Finite deformation and finite displacements are considered. Initial stress–strain state was performed as homogeneous equilibrium state in the infinite layer under weight forces. At time $t = 0$ suddenly a free surface, inclined to the horizontal base of slope on angle β appears.

The initial stress state in the material is

$$t = 0\ ,\ \sigma_{11} = -\frac{\lambda}{\lambda + 2\mu}\varrho g h\ ,\ \sigma_{22} = -\varrho g h\ .$$

where g is the acceleration of gravity.

Left and upper boundaries are free. We denote β the angle between the left boundary and vertical line. Horizontal foundation is fixed or free sliding. On the right side of the slope the non–reflection conditions were posed.

The material of the slope is described by two models: Drucker–Prager's model [47] and the elastic plastic model with micro–voids, suggested above.

In the case of Drucker–Prager's yield condition[47] instead of (1.6) we have

$$s_0^a = k_s - a\sigma_{kk}^a$$

and following law for bulk plastic strain rate

$$\dot{\varepsilon}_{kk}^p = a\Lambda_p\ ,$$

The elastic modules are $\mu = 35.65k_s$, $\lambda = 71.26k_s$. Drucker–Prager's parameter a has value between $a = 0$ (perfectly plastic material) and $a = 0.15$ (dense sand), $\tilde{h} = \frac{k_s}{g\varrho} \in [5, 15]$, the angle of slope was $\beta \in [\frac{\pi}{3}, \frac{\pi}{2}]$.

4.2. Method of solution

The problem was solved by the finite difference method on the moving Lagrange mesh. The explicit divergent scheme of second order of accuracy in space and time was employed [59].

4.3. Results

When a new free surface appears the unloading wave propagates and reflects from the boundaries of the domain. In result the equilibrium state is violated, the plastic deformations arise in the low part of the slope in the vicinity of the angle between the free surface and the rigid foundation and then the plastic zone develops as a rather narrow band towards the upper free surface.

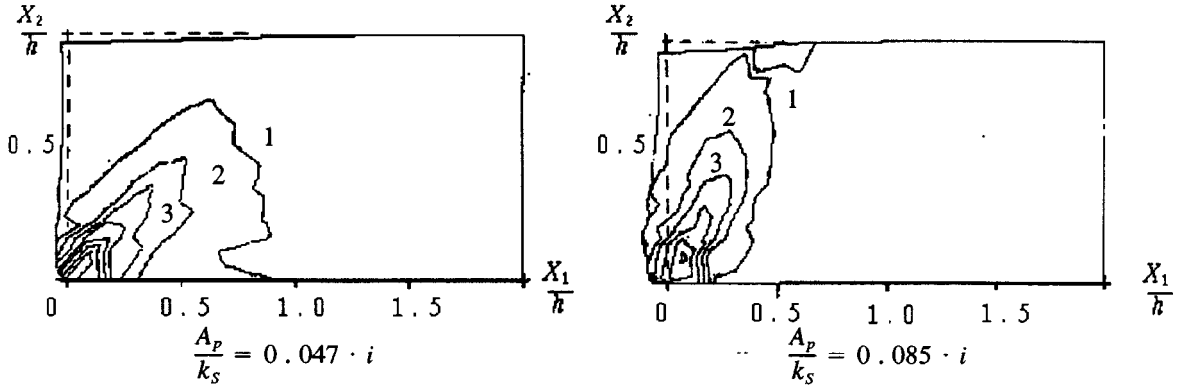

Figure 4.1 The influence of the internal friction on the contour lines of the plastic work:
a) $a = 0$, $h = 6\tilde{h}$, $t = 2.6\tilde{t}$; b) $a = 0.15$, $h = 12\tilde{h}$, $t = 1.9\tilde{t}$.

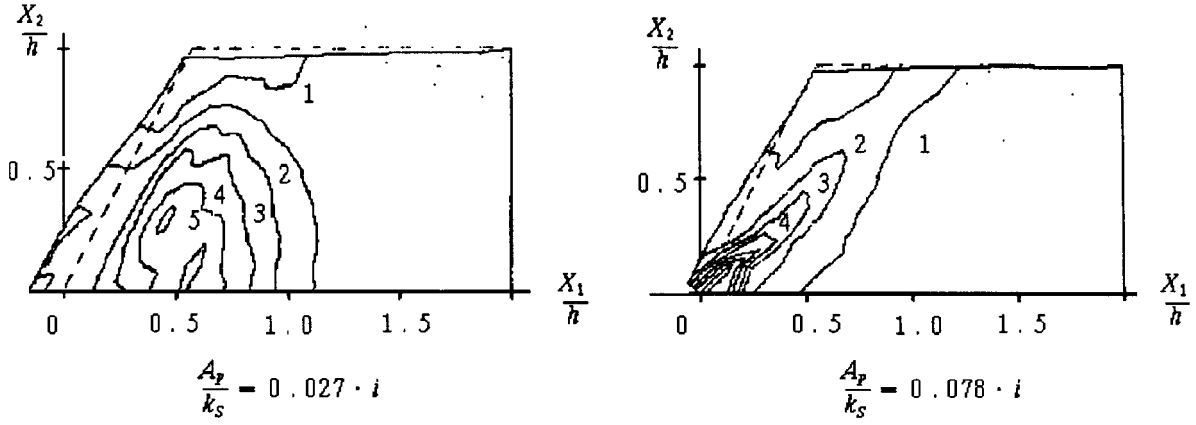

Figure 4.2 Different types of localization of plastic deformations:
a) sliding foundation $t = 2.3\tilde{t}$; b) fixed foundation $t = 4.3\tilde{t}$.

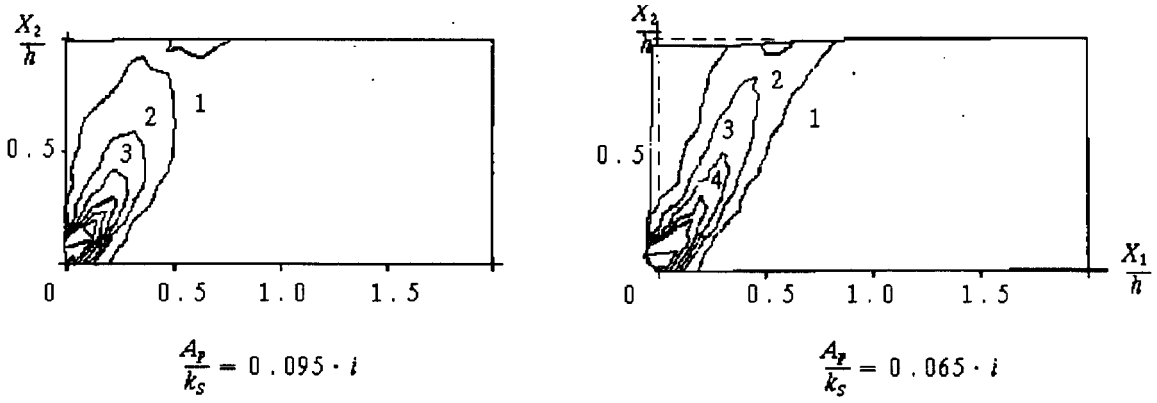

Figure 4.3 The localization of plastic deformations in model with micro–voids: $h = 12\tilde{h}$, $g_1 = 1$, $g_2 = 0.1$. Contour lines of plastic work: a) $t = 2.1\tilde{t}$; b) $t = 6.2\tilde{t}$.

Then the slope precipitates, its resistance exhausts and it slides down. This stage is close to the quasi–stationary process, where inertial forces are not significant.

The development of plasticity is shown by contour lines of plastic work A_p , where $\dot{A}_p = \sigma_{ij}\dot{\varepsilon}^p_{ij}$. On the Fig. 4.1a–4.1b the contour lines of A_p are shown ($\beta = \frac{\pi}{2}$, $\alpha = 0.01$ and $\alpha = 0.15$).

The patterns of deformation of the slope are also shown, and the initial position of the mass is indicated by dashed lines. It can be seen that the new plastic zone appears near the upper free surface and propagates towards the first zone due to tension caused by the precipitated slope . The angle between the plastic band and foundation is increasing with the parameter α . It is natural as α is connected with the internal friction angle ϱ by means of relation

$$\alpha = \frac{2\sin\varrho}{\sqrt{3}(3-\sin\varrho)} \ , \ k_s = \frac{6K\cos\varrho}{\sqrt{3}(3-\varrho)} \ , \tag{4.12}$$

where K is a coefficient of cohesion [47] in Coulomb–Mohr criterion

$$\tau_{\max} = K - \sigma_n tg\varrho \tag{4.13}$$

The localization depends also on the height of the layer h – the localization begins earlier for larger h and for smaller α . The comparison of the results for sliding and fixed foundation are given on Fig. 4.2. In the case a) the localization is not profound.

On Figure 4.3 the results for the model with micro–voids are given for different times. The parameters of the material $\nu = \frac{1}{3}$, $\lambda = 868k_s$, $\mu = 434k_s$, $h = 12\tilde{h}$, $g_1 = 1$, $g_2 = 0.1$ were chosen close to slightly strain softening material. The qualitative picture of the development of localization process is similar to the Drucker–Prager's model. The difference is quantitative, localization across the band for voided material is more distinct.

It should be mentioned that after the two zones of plastic deformation propagating towards each other are joined, the velocities of the particles increase and then a stage of steady state motion a

post–failure process begins . The study of results shows that for large post–failure displacements the spin components and rotations of the particles are large and that causes a growth of the zones of large gradients. The process again becomes unsteady and localization are not observed (Figures 4.7–4.8).

The conclusion can be made that for localization the steady state conditions are necessary. Another note should be made concerning to the numerical integration on the Lagrangian mesh. It is possible to use it in non–stationary problems until the deformation are of the order of unity then the accuracy is lost and other methods should be used [53,54]. So the suggested method is acceptable for moderate deformations.

5. The stability of slope under dynamical loading.

Localization of plastic deformation under dynamical loads in damaged materials is a subject of very intensive research during last years [32,33,37,57] (see also **Introduction**) . This interest is connected with the importance of dynamic fracture and failure of plastic and semi–brittle materials and also with the development of ideas in static localization problems.

5.1. Formulation of problem.

Here we study the dynamic localization process in the slope under the force and moment applied to the rigid punch in contact with the mass. The gravity forces are neglected.

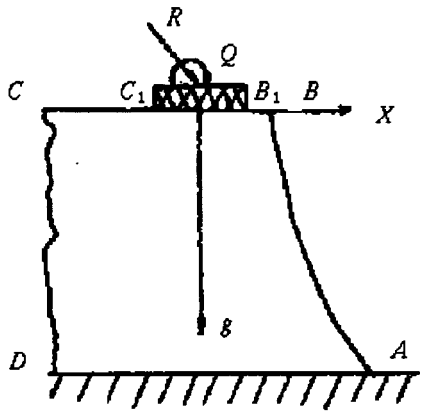

Figure 5.1 Stability of slope under dynamic loading

The dependence of elastic modules on the damage is taken from [65] as

$$\mu = \mu_0 e^{-\beta D} , \quad \lambda + 2\mu = (\lambda_0 + 2\mu_0) e^{-\alpha D} . \tag{5.4}$$

$$\dot{D} = \frac{1}{\tau_p s_0^a} (S^a - s_0^a)_+ . \tag{5.4}$$

where $D = \varepsilon^p_{kk}$.

5.2. Boundary conditions

Boundaries AB, BB_1 and CC_1 are free. The basement AD is fixed or sliding. On the left side boundary CD non–reflection conditions are used [4].

The punch is loaded by impulsive force and moment and rigidly connected with the slope along the contact line B_1C_1. Dimensionless approximation of the boundary conditions under punch is

$$\dot{v}_x = R_x + \int_{-L/2}^{L/2} \sigma_{xy} dx \,, \tag{5.12a}$$

$$\dot{v}_y = R_y + \int_{-L/2}^{L/2} \sigma_{yy} dx + xQ_z + x \int_{-L/2}^{L/2} \sigma_{yy} x dx \,, \tag{5.12b}$$

where R_x and R_y are projections of external force, Q_z is the external moment, L is length of the punch.

5.3. Method of solution

The problem was solved by the finite difference method. In the internal points the explicit McCormak's scheme of second order of accuracy was employed [61]. Boundary points were integrated on the base of bi–characteristic relations [62], this procedure ensures high accuracy of the calculations.

5.4. Results of calculations.

The results of calculations are presented on Fig. 5.3–5.8. Contour lines of function of damage D and field of the velocity directions for different values of time are shown. The punch was loaded by impulsive force and moment. The dependence of the force and the moment on time is shown in Fig. 5.2. The duration of the impulse was equal to the time of the elastic wave propagation along the length H. The values of the material constants are

$$\tau_p = 0.01 \,, \quad \frac{s_0^a}{\lambda_0 + 2\mu_0} = 0.02 \,, \quad \alpha = \beta = 10 \,, \quad \frac{2\mu_0}{\lambda_0 + 2\mu_0} = 0.33 \,.$$

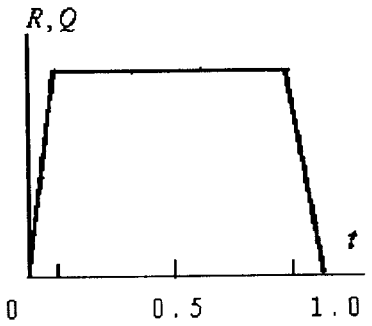

Figure 5.2 The dependence of external force and moment on time.

Maximal values of the dimensionless forces and the moment are
$R_x = 0$, $R_y = 0.04$, $Q = 0.02$.

On Figures 5.3–5.8 we can observe a very interesting picture of damage localization along the band which appears under the right side corner of the punch and propagates to the foundation of the slope in almost vertical direction (Fig. 5.3a–5.8a). The pictures of the field of the velocity directions show that waves are reflected from the damaged band (Figures 5.3b–5.8b). This can be explained by the fact that inside of a band the material is softened and has lost its rigidity, as follows from constitutive equations. The reflected waves cause tension in horizontal direction and the stress state in the vicinity of the band becomes close to pure shear state. According to the damage equation it leads to the increase of rigidity and to progressive damage localization. The part of slope between the localization band and free surface can separate from the remaining part and a new free surface will appear. Analogical situation could be repeated near the other corner of the punch, if the energy of the applied impulse would not dissipate at this time(Fig. 5.7a,5.7b).

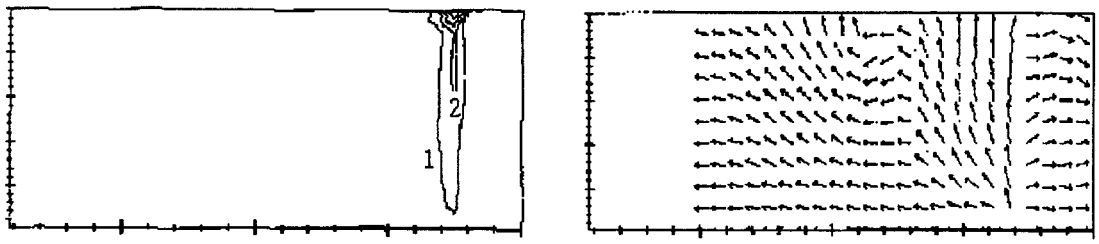

Figure 5.3. Case of sliding contact. a) Contour lines of function D , b) Velocity field. $t = 2$; $D_i = i \cdot 0.042$.

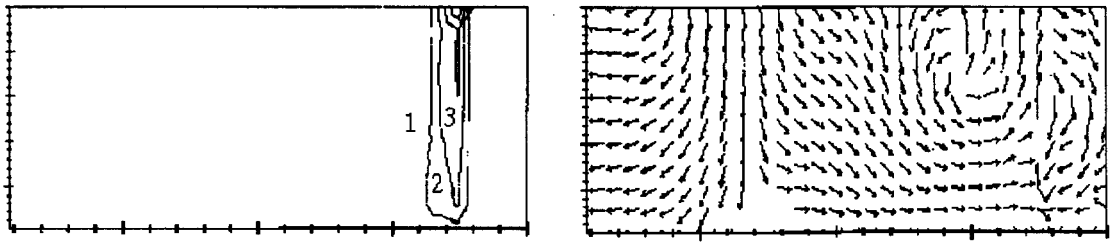

Figure 5.4. Case of sliding contact. a) Contour lines of function D , b) Velocity field. $t = 4$; $D_i = i \cdot 0.058$.

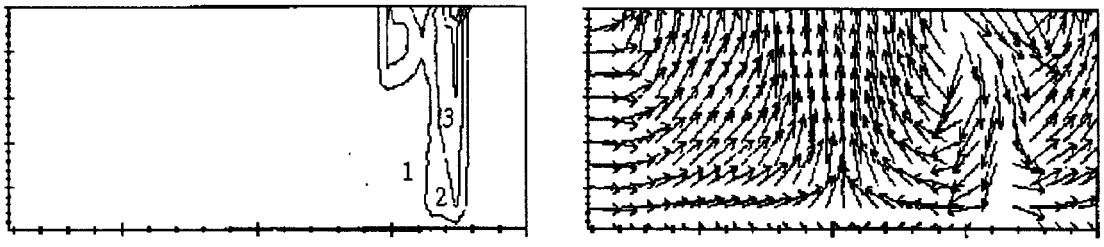

Figure 5.5. Case of sliding contact. a) Contour lines of function D , b) Velocity field. $t = 6$; $D_i = i \cdot 0.058$.

Comparison was made between two contact conditions on the base boundary. The results (see Fig. 5.6,5.7) show that there is no big difference in localization between fixed and smoothed con-

tact conditions (5.7a) and (5.7b). For fixed contact the localization is expressed more profoundly, the damage level is little higher than for smooth contact and the band is closer to the free surface.

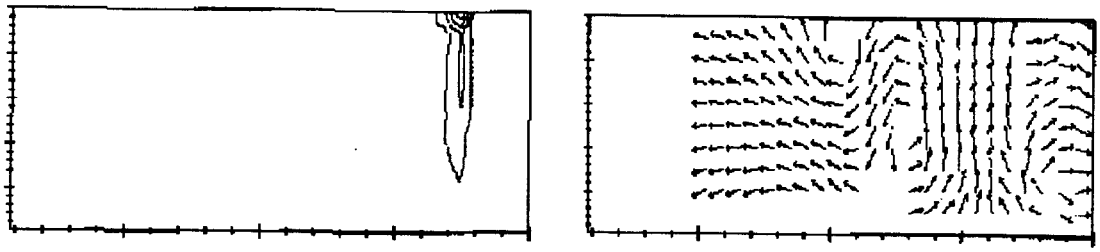

Figure 5.6. Case of fixed contact. a) Contour lines of function D , b) Velocity field. $t = 2$; $D_i = i \cdot 0.042$.

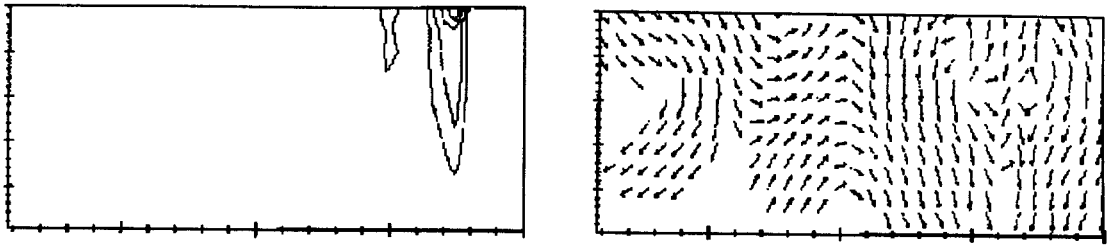

Figure 5.7. Case of fixed contact. a) Contour lines of function D , b) Velocity field. $t = 4$; $D_i = i \cdot 0.062$.

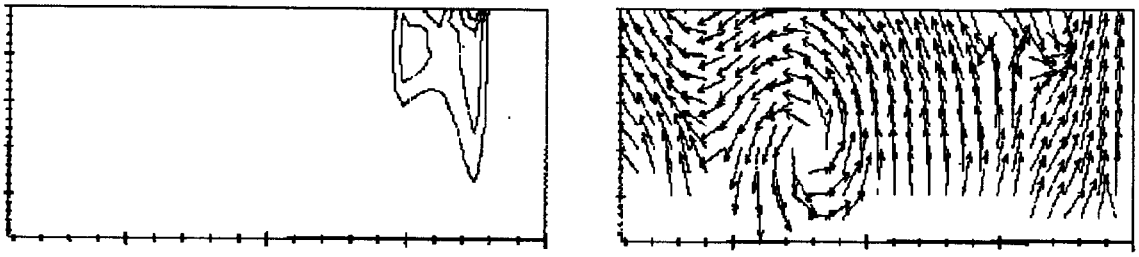

Figure 5.8. Case of fixed contact. a) Contour lines of function D , b) Velocity field. $t = 6$; $D_i = i \cdot 0.062$.

The picture of damage localization is very stable in wide range of the damage and relaxation factors. We can see also the strong influence of the boundary conditions on the localization.

6. The localization of strains in the extended specimen.

Let us see what will happen with a specimen, which is shown in Fig. 6.1., when it is subjected to slow extension and its right vertical boundary moves to the right with a permanent veloc-

ity $v_x = 0.0001 \ll c = 1$ (c −sound velocity). The material of the specimen has the following properties:

$$K = \frac{975}{(1+D)}, \quad \mu = \frac{369}{(1+D)}, \quad k_y = \frac{1}{(1+D)}, \tag{8.1}$$
$$c^2 = 1, \quad \dot{D} = 10^3 F, \quad F = (\varepsilon_{\max} - 0.001)_+ .$$

where $\varepsilon_{\max}$ is a maximal principal strain, $c^2 = \frac{(\lambda_0 + 2\mu_0)}{\varrho}$.

Finite element computer code "ASTRA" [69] is used for calculations. The FE grid and the behavior of the some functions at the beginning of the process are shown in Figures 6.1–6.2. At the corner we can observe the concentration of the strains and stresses which is the starting reason for the development of the damage. When the damage criterion $F > 0$ is fulfilled then the kinetic equation for the damage D begins to work. We can observe the propagation of the narrow band of the damage in Fig. 6.3 where the some kind of the strong discontinuity can be seen. The graphs of the horizontal displacement, mean stress, maximal principal strain and the damage function across the discontinuity are shown in Fig. 6.4–6.5.

The propagation of the discontinuity is essentially the dynamic process. It becomes clear from the history of the time step shown in Fig.6.5. Until the damage process starts the time step

$$\Delta t \leq \frac{\Delta \varepsilon_{\max}}{\|e\|} .$$

is much more than the dynamic time step

$$\Delta t_{dyn} \leq \frac{\Delta h}{c} .$$

When the damage process takes place the value of the actual time step very fast tends to the value of the dynamic time step which means that initially quasi–static process becomes to be a dynamic. To make the accurate and successive calculations one should take this fact into account.

The history of stress (Fig. 6.5) shows the physical instability of the process (the decrease of the stress while the strain increases). The distributions of the contour lines at the end of the process when the discontinuity reaches the opposite side of the specimen are shown in Fig. 6.6–6.7. We can see that finally the specimen is fractured into three parts.

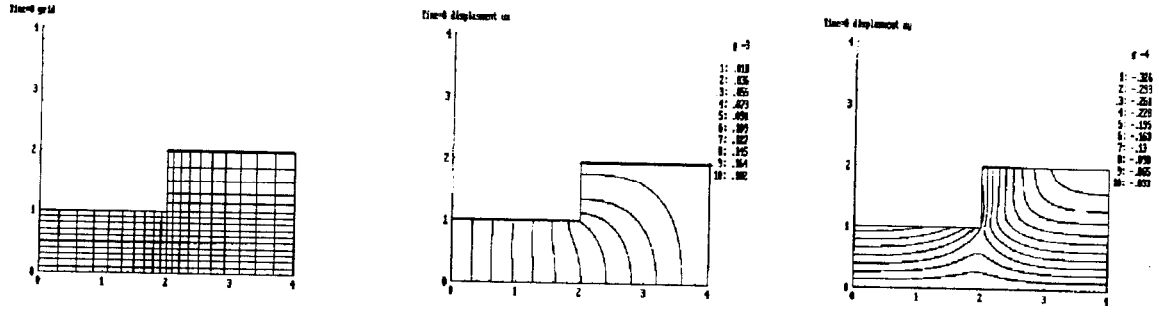

Fig. 6.1 Extension of the specimen. FE grid and distribution of the displacements at the beginning of the process.

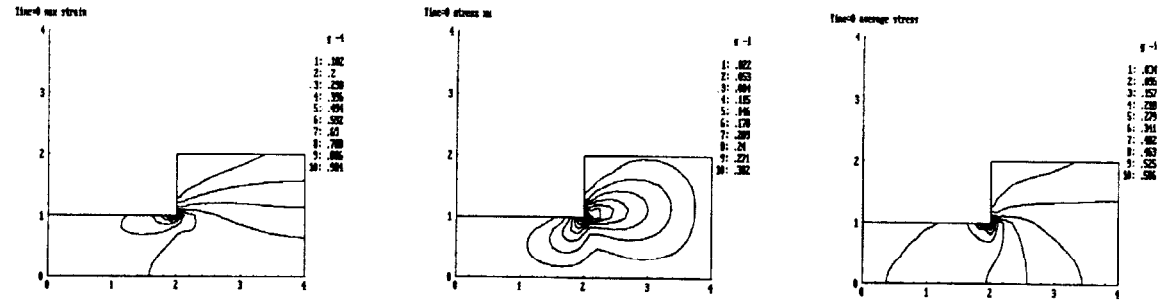

Fig. 6.2 Extension of the specimen. The distribution of maximal principal strain and stresses at the beginning of the process. The concentration of strains and stresses in the corner.

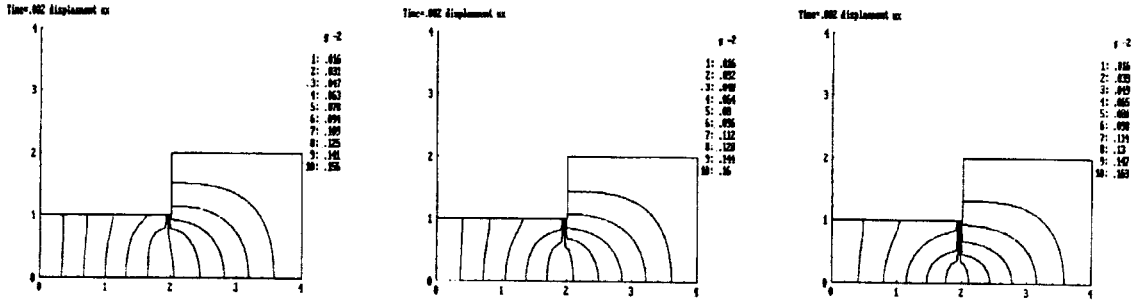

Fig. 6.3 Extension of the specimen. Development of the damage.

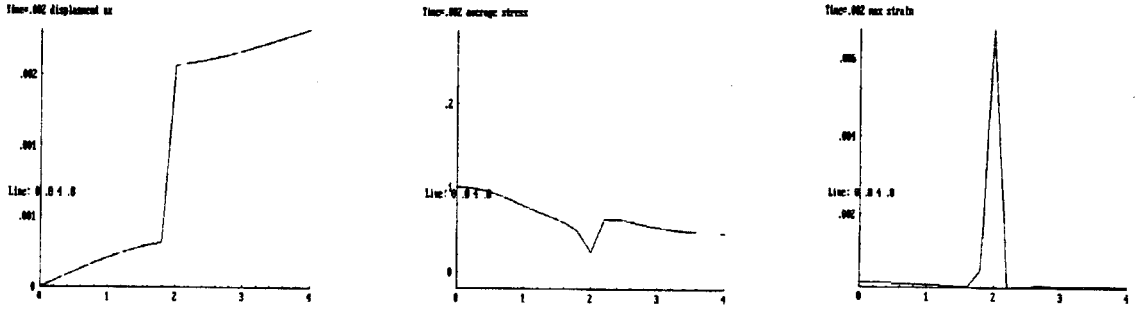

Fig. 6.4 Extension of the specimen. Graphs of the horizontal displacement, mean stress and maximal principal strain across the "discontinuity".

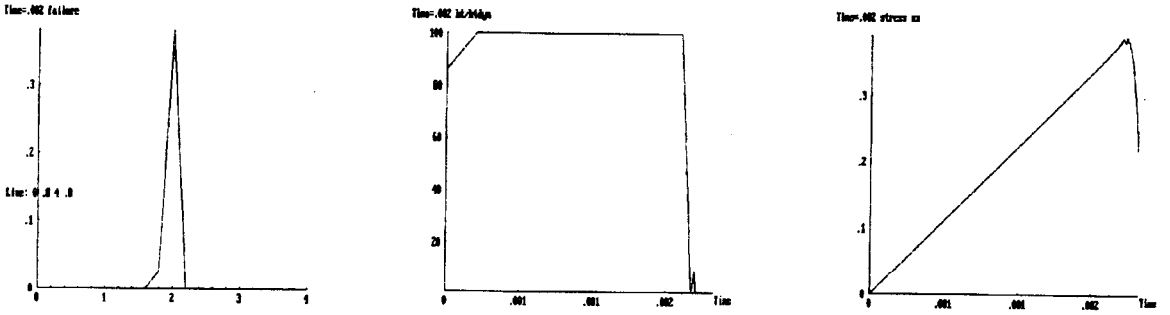

Fig. 6.5 Extension of the specimen. Graph of failure across the "discontinuity". History of the time step and stress.

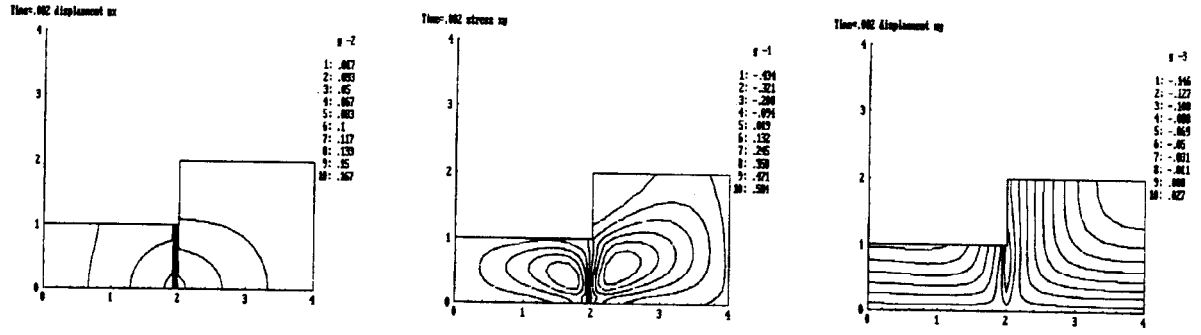

Fig. 6.6 Extension of the specimen. Horizontal displacement, share stress and vertical displacement for the end of process.

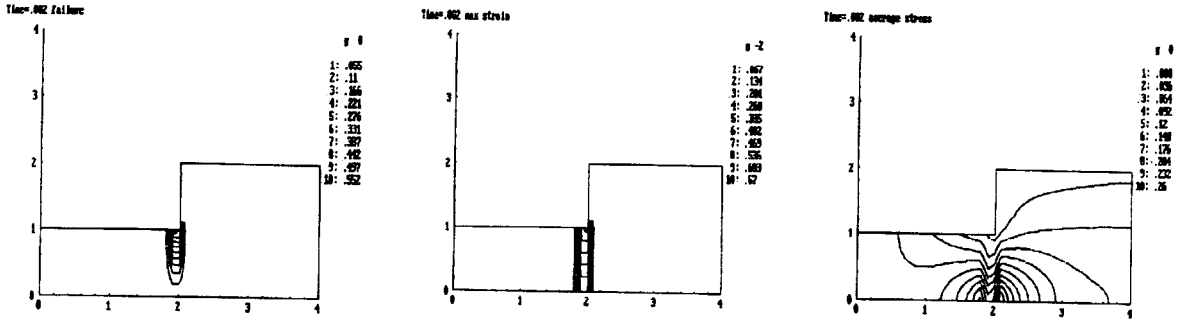

Fig. 6.7 Extension of the specimen. Failure function, maximal principal strain and mean stress for the end of process.

7. The localization of strains in an elastic plastic plate under a punch.

The elastic viscous plastic plate is loaded by the rigid punch which moves down slowly with permanent velocity (see Fig.7.1). Sliding contact conditions were used at the basement and under punch.

The properties of the material were

$$K = \frac{975}{(1+D)}\ , \quad \mu = \frac{369}{(1+D)}\ , \quad k_y = \frac{1}{(1+D)}\ , \tag{7.1}$$
$$c^2 = 1\ , \quad \dot{D} = 10^3 F\ , \quad F = (\varepsilon_{\max} - 0.01)_+\ .$$

The deformed grid and velocity field are drown in fIg.7.1. Contour zones of maximal principal strain and the failure function defined by relation

$$\tilde{\theta} = 1 - \frac{1}{1+D}\ , \quad 0 \le \tilde{\theta} \le 1\ ,$$

are shown in Fig.7.2. Strong localization of strains can be observed in all pictures. Finally the plate is fractured into three parts.

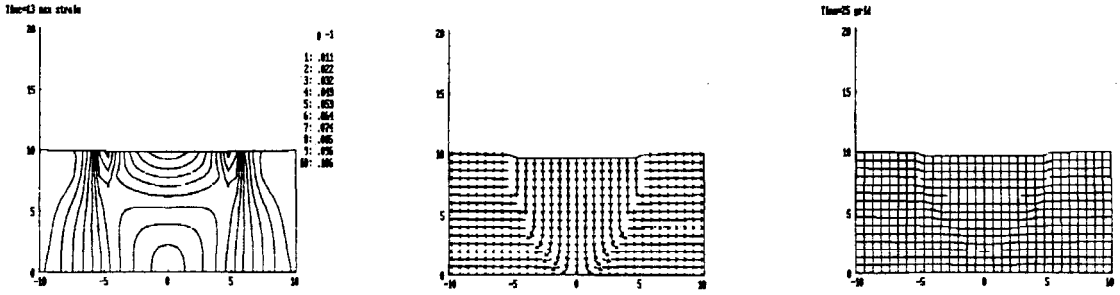

Fig. 7.1. Localization of strains under punch. Distorted grid (a) ,velocity field (b) and distribution of the maximal principal strain at the beginning of the process (c).

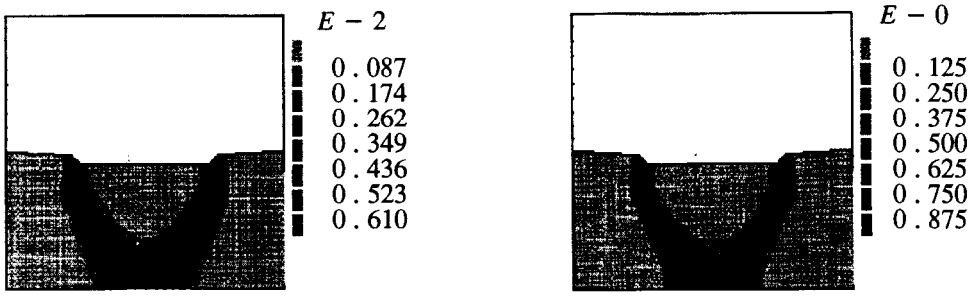

Fig. 7.2. Localization of strains under punch. Contour zones of maximal principal strain (c) and failure (d) at the end of the process.

8. The damage of collided elastic plastic plates.

A plate–striker hits a plate–target with impact velocity $u_0/c = 0.2$, where c is a sound velocity. The striker had the dimensionless material properties (7.1). Properties of the target were

$$K = \frac{243}{(1+D)}, \quad \mu = \frac{92}{(1+D)}, \quad k_y = \frac{0.25}{(1+D)},$$
$$c^2 = 1, \quad \dot{D} = 10^6 F, \quad F = (\varepsilon_{\max} - 0.01)_+ .$$

Evolution of damage bands (black color zones) is shown in Fig. 1a–1f. Finally the target is broken into three parts moving independently. The projectile is reflected and fully destroyed.

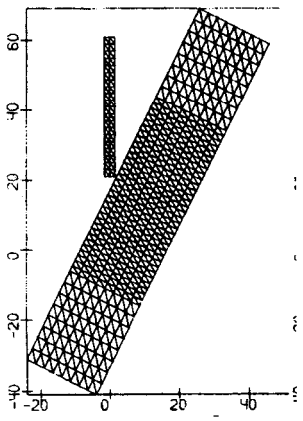

Fig. 8.1 Finite element grid

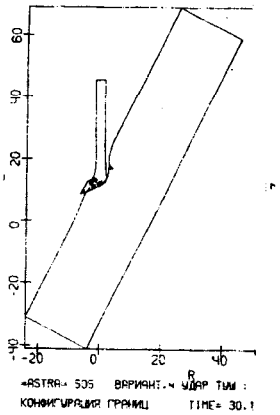

Fig.8.1 Evolution of impact

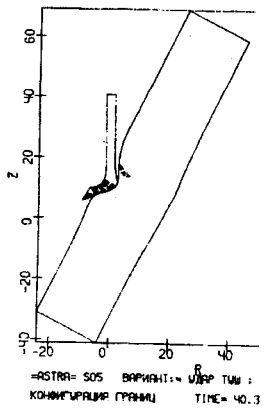

Fig. 8.3 Evolution of impact

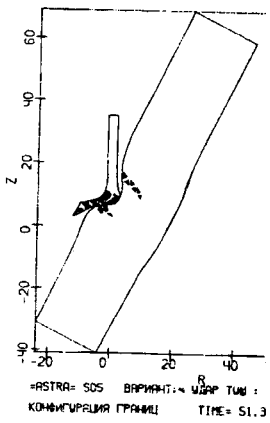

Fig. 8.4 The damage process

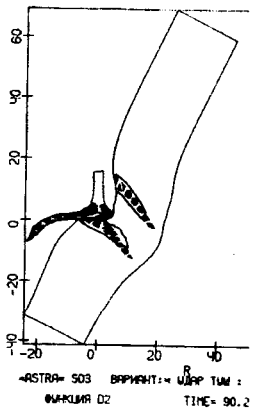

Fig. 8.5 The damage process

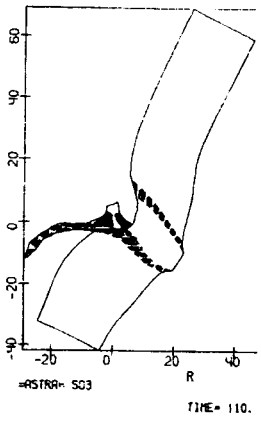

Fig. 8.6 Fractured configuration

9. Conclusion

Presented results are far from complete. Only the simplest modifications of the model are considered. Many questions of numerical simulation should be considered in future: mesh refinement and spurious effects, comparison between strain rate sensitive and non–sensitive models etc. However obtained results allow to make the conclusion that the suggested micro–mechanical model has some advantages before the strain–softening model as well as the Gurson's model and its modifications. It can describe the localization of plastic deformation and remove some drawbacks in other models.

10. Acknowledgment

The authors are very glad to acknowledge the Department of Structural Mechanics of Chalmers University of Technology and Swedish Royal Academy of Science for the support of our investigations within the project "Simulation of high rate technological processes" .

Great thanks we direct to Professor Alf Samuelsson for his tolerance, help, discussions, advises and corrections.

11. References

1. R. Hill, A general theory of uniqueness and stability in elastic–plastic solids. J. Mech. Phys. Solids, 6, 236–249, (1958).

2. J. W. Rudnicki and J. R. Rice, Conditions for the localization of deformation in pressure–sensitive dilatant solids. J. Mech. Phys. Solids, 23,371–394, (1975).

3. J. G. M. van Mier, Mode fracture of concrete: discontinuous crack growth and crack interface grain bridging. Cement and Concrete Research, 21, 1–15, (1991).

4. V. N. Kukudzanov, Numerical simulation dynamic processes of deformation and fracture in elastic plastic media. Uspechi Mechaniki, v.8,No.4, 21–65, (1995), (in Russian).

5. N.S. Ottosen and K. Runesson, Properties of discontinuous bifurcation solutions in elasto–plasticity. Int. J. Solids and Structures. vol. 27,No.4, 401–421, (1991).

6. M. A. Criesfield, Local instabili ties in the non–linear analysis of reinforced concrete beams

and slabs. Proc.Instn.Civ.Engrs,Part 2,73,135–145, (1982).
7. R. de Borst, Continuum models for localized failure. FEM–94, Non–linear and time dependent problems, Ed. N.E.Wiberg,19–34, (1994).
8. S. Pietruszczak and Z. Mroz, Finite element analysis of deformation of strain softening materials. Int. J. Num.Meth.Eng.,17,327–334, (1981).
9. Z. P. Bazant and B. Oh, Crack band theory for fracture of concrete. RILEM Materials and Structures, 16, 155–177, (1983).
10. Z. P. Bazant and T. Belitchko, Wave propagation in Strain Softening Bar: Exact Solution. ASCE J. of Eng.Mech., v.3, No 3., (1985).
11. R. Hill, A self–consistent mechanics of composite materials. J Mech. Phys. Solids, 13, 213, (1965).
12. G. Pijaudier–Cabot and Z. P. Bazant, Non–local damage theory. ASCE J. of Eng. Mech., 113, 1512–1533, (1987) .
13. E. C. Aifantis, On the micro–structural original of certain inelastic models. J. Eng. Mater. Technol.,106,326–334, (1984).
14. J. M. Duva and J. W. Hutchinson, Constitutive potentials for delutely voided nonlinear materials, 3, 41 (1984).
15. R. de Borst and H.–B. Muhlhaus, Gradient–dependent plasticity: formulation and algorithmic aspects. Int. J. Num. Meth. Eng.,35,521–539, (1992).
16. H.–B. Muhlhaus and I. Vardoulakis, The thickness of shear bands in granular materials. Geotechnique, 37,271–283, (1987).
17. R. de Borst, A generalization of J_2 –flow theory of polar continua. Comp. Meth. Appl. Mech. Eng.,103,99–122, (1993).
18. J. W. Hutchinson and K. W. Neale, Influence of strain rate sensitivity on necking under uniaxial tension. Acta Metall.,25, 839–846, (1977).
19. A. L. Gurson, Continuum theory of ductile rupture by void nucleation and growth. I. Yield criteria and flow rules for porous ductile media. J.Eng.Materials Technol.,99,2–15, (1977).
20. B. Budianski, J. W. Hutchinson and S. Stutski, Void growth and collapse in viscous solids. Mech of Solids., Ed. Hopkins, Pergamon Press,13–45. (1982)
21. J. B. Eshelby, The deformation of the elastic field of an ellipsoidal inclusion and related problems. Proc. Roy.Soc., A241, 376–392, (1957).
22. A. A. Movchan, Phenomenological description of dislocation mechanism of nucleated defects of plastic flow. J.Mech. i Tech. Physics, No.1,147–155, (1987) (in Russian)
23. R. Hill, The essential structure of constitutive laws for metal composites and polycrystals. J.mech.Phys.Solids, 15, 79–95, (1967).
24. F. McClinlock, A criterion for ductile fracture by growth of holes. J Appl. Mech. 35, 363–375, (1968).
25. B. Budiansky, On the elastic module of some heterogeneous materials. J Mech. Phys. Solids, 13 223–237, (1965).
26. G. Le Roy, J. D. Embury, G. Adward, M. F. Ashby, A model of ductile fracture on the nucleation and growth of voids, Acta Met., 29,1509–1521, (1981).
27. J. Barnby, Y. W. Shi and Z. Nadkarny, On the void growth during plastic deformation. Int. J. Fract.,29,No.4, 273–283, (1984)
28. G. M. Ljachov, Foundations of dynamics of explosive waves in soils and rocks. Nauka, Mos-

cow, (1974), (in Russian).
29. V. V. Adushkin, E. M. Platonov and N. M. Syrnikov, Mechanics of soil slopes. Fiziko–technicheskie problemy razrabotki poleznych iskopaemych, No.6, 71–80, (1971) (in Russian).
30. A. Needleman and J. R. Rice, Limits of ductility set by plastic flow localization. in Mechanics of Sheet Metal Forming (Eds. D.P.Koistinen et al.),Plenum Publishing Corporation, 237 267,(1978) .
31. M. Ortiz, Y. Leroy, and A. Needleman, A finite element method for localized failure analysis. Comput. Meth Appl.Mech.Engng, 61, 189–214, (1987).
32. V. N. Kukudzanov, On numerical simulation non–stationary processes of deformation and damage elastoplastic bodies under finite strains. in Math. Meth. of Mech. of Solids, Nauka, Moscow,75–85, (1986), (In Russian).
33. V. N. Kukudzanov, A numerical method for solution of unsteady elastoviscoplastic problems at large strains. In Finite Inelastic Deformations – Theory and Applications, (Eds. D. Besdo and E.Stein) 289–299, Springer Verlag, (1992).
34. J. Pan, M. Saje and A. Needelman, Localization of deformation in rate sensitive porous plastic solids. Int. J. Fracture, 21, 261–278, (1983).
35. A. Needleman and V. Tvergaard, An analysis of dynamic, ductile crack growth in a double edge cracked specimen. Int. J. Fracture, 49, 41–67, (1991).
36. V. Tvergaard and A. Needleman, Analysis of the cup–cone fracture in a round tensile bar. Acta Metallurgica, 32, 157–169, (1984).
37. V. Tvergaard and A. Needleman, Elastoviscoplastic of Ductile Fracture, in Finite Inelastic Deformations – Theory and Applications (Eds D.Besdo and E.Stein), 3–14, Springer Verlag, (1992).
38. J. J. Gillman, J.J. Dislocations and Mechanical Properties of Crystals. J Appl. Phys., Rev., 21, 767, (1968).
39. V. N. Kukudzanov, One dimensional waves propagation in elastoviscoplastic bars, Proc of Appl. Math., Computer Center of AN USSR, Moscow, (1977), (in Russian).
40. A. J. Seger, Dislocations and mechanical properties of crystals, Metallurgija, Moscow, (1959), (in Russian).
41. V. N. Kukudzanov and K. Santaoja, Thermodynamics of dislocation model of plasticity with micro–defects, (in printing).
42. D. D. Ivlev and G. I. Bykovcev,Theory of hardening plastic medium. Nauka, Moscow, (1971), (in Russian)
43. R. Hill, A general theory of uniqueness and stability in elastic plastic solids, J. Mech. Phys. Solids, 6, 236–249, (1958).
44. G. I. Taylor and H. Quinney, The latent energy remaining in a metal after cold working. Proc. Royal Soc. London, A143, 307–326, (1934).
45. G. Duvaut, J. Lions, Inequalities in Mechanics and Physics, Nauka, Moscow, (1980), (in Russian)
46. V. V. Sokolovsky, Statics of granular media,(IV edition), Nauka, Moscow, (1991), (in Russian)
47. D. C. Drucker and W. Prager, Soil mechanics and plastic analysis on design, Quart. Appl. Math., v.10, 157–165, (1962).
48. S. S. Gregorijan, On foundations dynamics of soils, Prikl.Math.Mech.,v.24,No 6,42–53,

(1960).
49. O. C. Zienkiewicz and G. C. Nayak, Elastoplastic stress analysis: a generalization for strain softening. Int J. Numerical Math.Eng.v.5,113–135, (1972).
50. D. Owen and E. Hinton Finite elements in plasticity,Swansea,U.K., (1984)
51. T. Belitchko, J. Fish and B. E. Engleman, A finite element with embedded localization zones, Comp.Math.Appl.Mech.Eng.,70,59–89, (1988).
52. R. Larsson and K. Runesson, Discontinuous displacement approximation for capturing plastic localization, Int.J.Num.Meth.Eng.,v.36,2087–2105, (1993).
53. R. Larsson and K. Runesson, Cohesive crack models derived from localization of damage coupled to plasticity, (to be published).
54. M. Ortiz and J. J. Quigly, Adaptive mesh refinement in strain localization problems, Comp. Meth. Appl. Mech. Eng., 90, 781–804, (1991) .
55. V. N. Kukudzanov, Numerical methods of solution nonlinear problems of mechanics of solids, Moscow, Phys.Techn.Univ.,98pp., (1990), (in Russian)
56. P. F. Korotkov, Shear bands on slopes failure, Dokladi Ac.Sci.USSR,v.267,No. 4 ,818–822, (1982),(in Russian)
57. R. E. Goodman, Introduction to Rock Mechanics,John Wiley sons.,(1980)
58. A. I. Glushko and I. I. Nesheretov, On kinetic approach to rocks failure,Izvestija Ac.Sci.USSR,MTT,No.6,140–146, (1986), (in Russian)
59. G. Meinchen and C. Sack, Numerical method "Tensor". In Comp.Probl.in Hydrodynamics, Moscow,Mir,185–211, (1967).
60. A. I. Glushko, On an approach to failure of geo–materials, Izvestija Ac. Sci. USSR, MTT, No.3, 130–135, (1988).
61. McCormak Numerical method solution viscous compressible flows. AIAA, v.1, No.4, 114–123, (1983).
62. R. Courant, Partial differential equations, Moscow, Mir, (1962).
63. V. N. Kukudzanov, A. N. Kovshov, V. L. Ivanov and D. N. Schneiderman, Localization of plastic deformations on the slopes stability problem, Preprint of IPM of Russian Acad.Sci., No.472,Moscow,72pp., (1994) ,(in Russian).
64. A. G. Evans and B. M. Connor, Toughening of brittle solids by martensitic transformation. Acta Metall., 34, 761, (1986).
65. I. N. Gupta, Seismic velocities in rock subjected to axial loading up to shear fracture, J. Geophys. Res., 78, 29, 6936–6942, (1973).
66. B. V. Zamyshliayev and L. S. Yevterev, Models of dynamic deformation and failure for ground media, Nauka, Moscow, 215 pp., (1990), (in Russian).
67. V. N. Kukudzhanov, Investigation of shock wave structure in elastic visco plastic bars using the asymptotic method. Arch. Mech., 33, 5, 739–751, (1981).
68. F. McClintock, S. Kaplan and C. Berg, Fracture by hole growth in shear, Int. J. Fracture Mech., 2, 4, 614–627, (1966).
69. N. G. Bourago, Computer code "ASTRA" for nonlinear problems in continuous mechanics, in "Abstracts of the 7th Nordic Seminar on Comput.Mech.", Trondheim, 1994.